

**ZINC SPECIATION OF A SMELTER CONTAMINATED  
BOREAL FOREST SITE**

A Thesis Submitted to the College of  
Graduate Studies and Research  
In Partial Fulfillment of the Requirements  
For the Degree of Master of Science  
in the Department of Soil Science  
University of Saskatchewan  
Saskatoon

By

Jordan Graeme Hamilton

## **PERMISSION TO USE**

In presenting this thesis in partial fulfilment of the requirements for a Postgraduate degree from the University of Saskatchewan, I agree that the Libraries of this University may make it freely available for inspection. I further agree that permission for copying of this thesis in any manner, in whole or in part, for scholarly purposes may be granted by the professor or professors who supervised my thesis work or, in their absence, by the Head of the Department or the Dean of the College in which my thesis work was done. It is understood that any copying or publication or use of this thesis or parts thereof for financial gain shall not be allowed without my written permission. It is also understood that due recognition shall be given to me and to the University of Saskatchewan in any scholarly use which may be made of any material in my thesis.

Requests for permission to copy or to make other use of material in this thesis in whole or part should be addressed to:

Head, Department of Soil Science  
University of Saskatchewan  
51 Campus Drive  
Saskatoon, Saskatchewan S7N 5A8

## ABSTRACT

HudBay Minerals (formerly the Hudson Bay Mining and Smelting Co., Limited) has operated a Zn and Cu processing facility in Flin Flon, MB since the 1930's. Located in the Boreal Shield, the area surrounding the mine complex has been severely impacted by both natural (forest fires) and the anthropogenic disturbance, which has adversely affected recovery of the local forest ecosystem. Zinc is one of the most prevalent smelter-derived metals in the soils and has been identified as a key factor limiting natural revegetation of the landscape. Because metal toxicity is related more to speciation than to total concentration, Zn speciation in soils from the impacted landscape was characterized using X-ray absorption fine structure, X-ray fluorescence mapping and  $\mu$ -X-ray absorption near edge structure. Beginning with speciation at a micro-scale and transitioning to bulk speciation was able to determine Zn speciation and link it to two distinct landform characteristics: (1) soils stabilized by metal tolerant grass species—in which secondary adsorption species of Zn (i.e., sorbed to Mn and Si oxides, and as outer-sphere adsorbed Zn) were found to be more abundant; and (2) eroded, sparsely vegetated soils in mid to upper slope positions that were dominated almost entirely by smelter derived Zn minerals, specifically Franklinite ( $\text{ZnFe}_2\text{O}_4$ ).

The long-term effect of liming on pH and Zn speciation was examined using field sites limed by a community led organization over a ten year period. Upon liming to a pH of 4 to 4.5, the eroded, sparsely vegetated soils were found to form a Zn-Al-Hydroxy Interlayer Material (HIM) co-precipitate, reducing the phytotoxicity of both Zn and Al and allowed for boreal forest vegetation to recovery quickly in these areas. The grass stabilized soils experienced a steady pH increase, as compared to a sporadic pH increase in the heavily eroded soils, as the buffering capacity was overcome allowing for a transition between multiple adsorption species based upon the point of zero charge of reactive soil elements. Ultimately reaching a near neutral pH after ten years, this allowed for the formation of stable Zn-Al-layered double hydroxide (LDH) soil precipitates and significantly reduced concentrations of plant available Zn.

## ACKNOWLEDGMENTS

I would like to thank my supervisors Drs. Derek Peak and Richard Farrell for all their help throughout the research and writing process. I greatly appreciate the extra patience of Dr. Derek Peak for his help and understanding throughout the learning process with synchrotron based X-ray absorption spectroscopy, without which I would not be where I am today. I would also like to thank my advisory committee members, for all their time and help given throughout this research, Dr. Steven Siciliano and Dr. Jeff Warner, as well as my external examiner, Dr. Matt Lindsay.

I could not have completed this research without the help and support of my fellow students involved with the Flin Flon/Creighton revegetation project: Jen, Courtney, Aaron, Cass, Katlin, Amanda, and Catlan. I would also like to thank the Canadian Light Source (CLS) Synchrotron and more specifically the VESPERs and HXMA beamline staff for their time and effort to teach me how to troubleshoot and optimize their beamlines, making the data collection process much less stressful. I would also like to thank my girlfriend Stephanie and my family for the support they provided, I would not have been able to complete this work without them.

I would like to thank HudBay Minerals, Inc. and the *Flin Flon/Creighton community Green Project* for their collaboration throughout this research. This research was funded by a Natural Science and Engineering Research Council (NSERC) Collaborative Research and Development (CRD) grant with HudBay Minerals Inc. (formerly Hudson Bay Mining and Smelting Co., Limited).

## TABLE OF CONTENTS

	<u>Page</u>
<b>ABSTRACT .....</b>	<b>II</b>
<b>ACKNOWLEDGMENTS.....</b>	<b>III</b>
<b>LIST OF TABLES.....</b>	<b>VI</b>
<b>LIST OF FIGURES.....</b>	<b>VII</b>
<b>LIST OF ABBREVIATIONS.....</b>	<b>IX</b>
<b>1 INTRODUCTION.....</b>	<b>1</b>
<b>2 LITERATURE REVIEW .....</b>	<b>4</b>
2.1 Soil properties influencing metal speciation.....	4
2.2 Zinc speciation and fractionation in soils .....	6
2.3 X-ray Absorption Spectroscopy.....	11
2.3.1 X-ray absorption spectroscopy techniques.....	12
2.3.2 XAS Linear combination fitting.....	13
2.3.3 X-ray microprobe ( $\mu$ XRF mapping and $\mu$ XANES) .....	14
<b>3 ZINC SPECIATION IN A SMELTER AFFECTED BOREAL FOREST ECOSYSTEM: SITE CHARACTERIZATION USING EXAFS SPECTROSCOPY..</b>	<b>17</b>
3.1 Preface .....	17
3.2 Introduction.....	17
3.3 Materials and Methods.....	19
3.3.1 Soils.....	19
3.3.2 Soil analysis.....	20
3.3.3 XAS data collection and analysis.....	22
3.4 Results and Discussion .....	23
3.4.1 XRF image maps and contaminant spatial distribution .....	23
3.4.2 Bulk Zn XAS speciation .....	25
3.4.3 Influence of soil erosion and slope position on Zn speciation .....	28
3.4.4 Zinc stability and environmental significance.....	34
3.5 Conclusions.....	35

<b>4</b>	<b>EFFECTS OF DOLOMITIC LIMESTONE APPLICATION ON ZINC SPECIFICATION IN A BOREAL FOREST SMELTER CONTAMINTED LANDSCAPE.</b>	<b>37</b>
4.1	Preface .....	37
4.2	Introduction.....	37
4.3	Materials and Methods.....	40
4.3.1	Site and soil selection .....	40
4.3.2	Carbonate and application methods .....	41
4.3.3	Soil analysis.....	41
4.3.4	XAS Data collection and analysis .....	42
4.4	Results and Discussion .....	43
4.4.1	Effect of dolostone application on soil pH.....	43
4.4.2	Zinc XAS speciation .....	45
4.4.3	Effect of liming on Chronosequence Zn speciation .....	51
4.4.4	Long term effects of liming on Zn phytotoxicity .....	52
4.5	Conclusions.....	53
<b>5</b>	<b>SYNTHESIS AND GENERAL DISCUSSION .....</b>	<b>55</b>
5.1	General Zn speciation in Flin Flon .....	55
5.2	High Erodibility Soils .....	57
5.2.1	Landscape effect on Zn speciation .....	57
5.2.2	Reducing Zn phytotoxicity in high erodibility soils.....	57
5.3	Stabilized/depressional Soils .....	58
5.3.1	Landscape effects on Zn speciation.....	58
5.3.2	Reducing Zn phytotoxicity in stabilized soils .....	59
<b>6</b>	<b>CONCLUSION.....</b>	<b>61</b>
<b>7</b>	<b>REFERENCES .....</b>	<b>64</b>
	<b>APPENDIX A.....</b>	<b>69</b>
A.1.	Precipitate standards.....	70
A.2.	Sorption standards .....	70
A.3.	Mineral standards .....	71
A.4.	Linear combination fitting rational.....	74
	<b>APPENDIX B.....</b>	<b>76</b>
	<b>APPENDIX C.....</b>	<b>81</b>

## LIST OF TABLES

<u>Table</u>	<u>page</u>
Table 3.1. Bulk soil chemical analysis and XAS Linear Combination Fit (LCF) <sup>†</sup> results for surface (0-2 cm) and subsurface (8-10 cm) soils.....	31
Table 4.1. Soil pH and CaCl <sub>2</sub> extractable concentrations of the chronosequenced liming sites. ....	44
Table 4.2. Bulk XAS LCF results of the chronosequence soil catenas.....	50
Table A.1. Loadings of Zn adsorption reference standards .....	71

## LIST OF FIGURES

<u>Figure</u>	<u>page</u>
Fig. 2.1. Example of linear combination fitting (LCF) modeling of a bulk EXAFS soil sample from Flin Flon. Experimental data is shown in black with + symbols, the best fit LCF model is shown in red, and the 3 standard components (Zn-Al-HIM, franklinite, and Zn adsorbed on a smectite clay) and their relative proportions are shown below the fit. ....	14
Fig. 2.2. Example results from an X-ray Microprobe experiment on a Flin Flon soil. (Left) X-ray fluorescence (XRF) intensity maps of Zn, Cu, Fe and Mn show the range of elemental concentrations in the sample. (Center) A tri-colour map of the XRF results indicating the relative concentrations of Zn, Fe and Mn and the co-location of these three elements. (Right) Zn K-edge $\mu$ XANES spectra from interesting spots in the sample (labeled on the tri-color map as (A-F) reveal differences in Zn speciation at the micro-scale.....	15
Fig. 3.1. Sampling sites used in characterizing Zn speciation in relation to the smelter/processing facility (Red). High erodibility (Orange) and stabilized (Green) soils are indicated with picture representations defining each classification. Aerial photo provided by University of Saskatchewan Department of Soil Science Soil Survey of Flin Flon, MB. ....	21
Fig. 3.2. Site 4 surface soil (0-2 cm) synchrotron XRF microprobe maps for Zn, Fe, Cu, and Mn. Colors denote intensity (red = relative high elemental concentration, dark blue = low relative elemental concentration) and tri-colour maps (500 $\times$ 500 $\mu$ m) reveal 2D spatial relationships of Zn, Fe, and Mn throughout the soil...	24
Fig. 3.3. Site 7 surface soil (0-2 cm) synchrotron XRF microprobe maps for Zn, Fe, Cu, and Mn. Colors denote intensity (red = high relative elemental concentration, dark blue = low relative elemental concentration) and tri-colour maps (300 $\times$ 300 $\mu$ m) reveal 2D spatial relationships of Zn, Fe, and Mn throughout the soil...	26
Fig. 3.4. Bulk Zn K-edge XANES (black lines) with LCF model fits (red lines) of surface (0-2 cm) and subsurface (8-10 cm) measurements of studied sites surrounding the Flin Flon, MB smelter. ....	29
Fig. 3.5. Bulk EXAFS with LCF model fits of surface (0-2 cm) and subsurface (8-10 cm) measurements of studied sites surrounding the Flin Flon, MB smelter. ....	30



Fig. 4.1.	Bulk Zn XANES of the high erodibility chronosequence soils. Experimental data is shown by black crosses, and the LCF results are shown with a red line. The dashed line at 9710 eV highlights a shoulder feature that is diagnostic for neo-phase Zn-Al-HIM precipitate. For comparison, a Zn-Al-HIM and franklinite standard are shown in blue.....	47
Fig. 4.2.	Bulk Zn $k^3$ -EXAFS (black) and LCF results (red) of the vegetation-stabilized chronosequence soil catena. The EXAFS of the “3 years since liming” spectra was limited to 9k ( $\text{\AA}^{-1}$ ) to ensure the LCF model wasn’t affected by signal quality. For reference, $k^3$ -EXAFS of franklinite are shown in blue, and dashed lines denote regions diagnostic for franklinite in the EXAFS spectra of the chronosequence soils. ....	48
Fig. 4.3.	Bulk Zn XANES of the vegetation-stabilized chronosequence soil catena. Experimental data is shown by black crosses, and the LCF results are shown with a red line. For comparison, a franklinite standard is shown in blue. ....	49
Fig. A.1.	Zinc reference standards, XANES spectra used in Linear Combination Fitting (LCF) of Flin Flon soil samples.....	72
Fig. A.2.	Zinc reference standards bulk EXAFS used in Linear Combination Fitting (LCF) of Flin Flon soil samples.....	73
Fig. B.1.	Core used to collect surface and depth soil throughout the Flin Flon MB landscape, 10 cm in total length. ....	77
Fig. B.2.	Site 1 landscape photo. The area is characterized by metal tolerant grass species limiting the potential for soil erosion. Much of the metal tolerant grass had been removed for the development of amendment plots. ....	78
Fig. B.4.	Site 3 landscape photo, area is characterized by high potential rates of soil erosion. This site is located approx. 1 km North and slightly east of the smelting and processing facility. ....	80
Fig. C.1.	Un-limed high erodibility surface soil (0-2 cm) synchrotron XRF microprobe maps for Zn, Fe, Cu, and Mn. Colors denote intensity (red = high relative elemental concentration, dark blue = low relative elemental concentration) and tri-colour maps ( $300 \times 300 \mu\text{m}$ ) reveal 2D spatial relationships of Zn, Fe, and Mn throughout the soil.....	82
Fig. C.2.	High erodibility ten years since liming surface soil (0-2 cm) synchrotron XRF microprobe maps for Zn, Fe, Cu, and Mn. Colors denote intensity (red = high relative elemental concentration, dark blue = low relative elemental concentration) and tri-colour maps ( $400 \times 400 \mu\text{m}$ ) reveal 2D spatial relationships of Zn, Fe, and Mn throughout the soil.....	83

## **LIST OF ABBREVIATIONS**

CEC	Cation exchange capacity
CLS	Canadian light source Synchrotron
EXAFS	Extended X-ray absorption fine structure spectroscopy
HXMA	Hard X-ray MicroAnalysis-Canadian Light Source beamline
LCF	Linear combination fitting
PZC	Point of zero charge
VESPERs	Very Sensitive Elemental and Structural Probe Employing Radiation from a Synchrotron
XAS	X-ray absorption spectroscopy
XAFS	X-ray absorption fine structure
XANES	X-ray absorption near edge spectroscopy
Zn-Al-LDH	Zinc aluminum layered double hydroxide
Zn-Al-HIM	Zinc aluminum hydroxy interlayer material

## 1 INTRODUCTION

The revegetation of contaminated mining and smelting sites has proven to be one of the most effective ways of stabilizing metal contamination and reducing erosion in impacted soils (Manceau et al., 2000; Roberts et al., 2002; Scheinost et al., 2002). Revegetation not only limits soil erosion and nutrient loss but also the accumulation of toxic metals in low-lying areas of the landscape. The scale of heavy metal contamination from smelting activities is generally too large to be remediated by *ex-situ* soil removal methods; *in-situ* revegetation strategies are therefore favored not only economically but also for their effectiveness (Khan and Jones, 2009). Immobilizing bare contaminated soils with plant cover provides several benefits that can result in reduced metal toxicity: soil stabilization increases contact time for metal sorption to soil surfaces (mineral and organic) and decreases water percolation to the water table. Both of which limit the transport of labile metals and provide conditions favorable for natural attenuation (Vespa et al., 2010). Accordingly, the challenge facing revegetation efforts is often how best to establish plant stands in areas that are contaminated with metals and/or are so highly eroded that the amount and quality of soil present is limiting to plant growth.

The copper-zinc mine and smelter complex in Flin Flon, MB (owned and operated by HudBay Minerals, Limited) has been in continuous operation since 1930. Although the smelter complex has been regularly upgraded to improve processing and meet environmental and regulatory standards, one of the long-term effects of smelter operations has been an increase in tree mortality from which the area has been extremely slow to recover. Several large forest fires and an extensive forestry industry have contributed to the loss of forest habitat, but inputs of heavy metals and acidity from the smelter facility have interfered with natural forest recovery. Indeed, the area surrounding the smelter complex in both Flin Flon, MB and Creighton, SK is characterized by a large expanse of deforested, heavy metal contaminated soil that has been severely eroded over time (Henderson et al., 1998).

Heavy metal toxicity often depends upon the speciation present in the environment, given there are sufficient total concentrations to produce toxic effects (Jacquat et al., 2009a). Thus, site-specific information on metal speciation is essential to the development of a successful revegetation strategy. Previous research in the area found total soil Zn levels in the low weight percent (500–20,000 mg Zn kg<sup>-1</sup>soil) range (Henderson et al., 1998), making it the most concentrated metal contaminant for this site. There is a high potential for Zn phytotoxicity at these concentrations depending upon the chemical species present throughout the rooting zone of the soil (Roberts et al., 2002). Detailed chemical speciation of Zn in soils from the Flin Flon site can potentially help explain how this metal currently affects existing vegetation and how to overcome any Zn-induced limitations to the overall success of the revegetation project.

Successful revegetation of the affected landscape will require new understanding of boreal forest ecosystems that have been heavily compromised by zinc contamination and soil acidification. Chemical speciation data from the Flin Flon, MB landscape will not only influence the management techniques of this revegetation project but also potentially be extended to other smelter contaminated sites. The scientific benefits of this research lie in characterizing Zn speciation and interactions with the soil environment in a smelter-affected boreal forest ecosystem, and how Zn speciation is influenced by both time and soil amendments designed to facilitate revegetation.

This thesis is presented in chapter format with Chapter 1 (Introduction) introducing the problem and rationale for my thesis research. Chapter 2 contains a detailed Literature Review of the existing work in the area of soil Zn speciation, provides a basis for the current research, and identifies gaps in the literature. This is followed by two research chapters, the first of which (Chapter 3) characterizes existing Zn speciation in the Flin Flon, MB landscape. The second research chapter (Chapter 4) looks at the effect of a gradual pH increase and time on Zn speciation in the Flin Flon, MB landscape at two sites: (1) a highly erodible soil and (2) and a metal tolerant grass stabilized soil. The chapter following the research chapter (Chapter 5) is a discussion of the overall synthesis of Zn speciation and interactions in the soil environment. Chapter 6 is an overall conclusions chapter regarding Zn speciation research in Flin Flon, MB and future research needs. A compilation of the references cited in Chapters 1-5 is provided in Chapter 7.

Additional information on the synthesis of the XAS Zn reference standards including the XANES and EXAFS spectra of all collected Zn reference materials can be found in Appendix A. Photos of the field sites described in Chapter 3 can be found in Appendix B. Appendix C contains supplemental information for Chapter 4, including additional methodology for the chapter.

## **2 LITERATURE REVIEW**

The toxicity of heavy metals in the environment has been well documented to be a product of both metal concentration and speciation, or chemical form of the metal (Alloway, 1995; Manceau et al., 2000; Basta et al., 2005; Jacquat et al., 2009a). This has been observed for Zn in a variety of smelter-contaminated soils (Manceau et al., 2000; Scheinost et al., 2002; Voegelin et al., 2011); moreover, Zn speciation can be related to Zn phytotoxicity by measuring the plant available fractions. Labile Zn species that do not form strong bonds with soil surfaces are not only transported more readily through the soil but are also more available for uptake by plants and microorganisms (Alloway, 1995). The labile metal fraction in soils will be influenced by the characteristics and properties of the soil as well as the speciation of the metal itself. Determining the speciation and associated phytotoxicity of heavy metals in soils has traditionally been determined by a set of operationally defined sequential extractions, specifically, as to which extraction step the metal was removed from the soil was linked to potential phytotoxicity (Alloway, 1995; Malandrino et al., 2011). Extractions for plant available metals are still widely used but are increasingly performed in conjunction with synchrotron-based X-ray absorption spectroscopy (XAS) techniques to directly measure speciation (Manceau et al., 2000; Julliot et al., 2003; Vespa et al., 2010). Determining the solid-state speciation in representative field samples is now recognized as an important part of any metal contamination project (Manceau et al., 2000; Jacquat et al., 2009a; Voegelin et al., 2011; Churakov and Daehn, 2012).

### **2.1 Soil properties influencing metal speciation**

Soil properties that influence metal speciation in soils include: pH, cation exchange capacity (CEC), soil organic matter content, soil mineralogy, and soil texture (Impellitteri et al., 2001). Whereas these properties generally reflect the soil forming factors in the area,

they can be significantly altered by human activity (Impellitteri et al., 2001). Soil pH influences soil properties and also significantly influences the speciation of heavy metals such as Zn (Alloway, 1995).

An acidic pH alters the soil environment in several ways; the first is that  $H^+$  will substitute onto the negatively charged soil particles displacing adsorbed metal cations, releasing them into solution (Alloway, 1995). An acidic pH also influences metals by protonating the functional groups of soil surfaces giving rise to positive surface charges (Alloway, 1995). Positively-charged soil particles have limited adsorption capacity for heavy metal (e.g.  $Zn^{2+}$ ) cations (Alloway, 1995). Boreal forest soils are naturally acidic; when combined with acidification arising from sulfur dioxide deposition from the smelting process the number of reactive exchange sites for Zn are greatly reduced (Augusto et al., 1998; Ek et al., 2001). The oxidation of aerially deposited metal sulphide minerals will further acidify the soil, reduce the number of exchanges sites, and increase the concentration of labile metals (Ek et al., 2001). Metals bonding directly to the surface functional groups of soil particles (inner-sphere adsorption) generally will have a greater sorption capacity and stability than metals held via cation exchange (outer-sphere adsorption), but adsorption processes are controlled by pH and limited in acidic conditions (Alloway, 1995).

Cation exchange capacity (CEC) is a measure of the soil's net negative charge and its ability to absorb positively charged cations, including  $Zn^{2+}$  (Alloway, 1995). A soil's CEC is dependent on several factors, including pH, and the type/amount of clay minerals and organic matter present in the soil (Impellitteri et al., 2001). The net negative charge of soil particles (CEC) is the result of both isomorphic substitution in clay minerals and pH dependent charge arising from deprotonation of both clay minerals and organic matter (Alloway, 1995). Isomorphic substitution is the substitution of a similarly sized atom into the lattice of the clay structure that has a lower positive charge eg.,  $Al^{3+}$  substitution for  $Si^{4+}$ ; this results in a net negative surface charge (Alloway, 1995). Variable or pH dependent charge occurs on the edge sites of minerals and on organic matter surfaces. Increasing solution pH causes deprotonation of functional groups on particle surfaces which results in a greater negative charge (Alloway, 1995). In general, the CEC of a mineral soil ranges from about 3 to 60  $cmol_c\ kg^{-1}$  of soil, whereas the CEC of organic

matter can exceed  $200 \text{ cmol}_c \text{ kg}^{-1}$  (Kingery et al., 2001). The CEC of organic matter is almost exclusively due to pH dependent charge and the sheer number of reactive functional groups (i.e., carboxyl and phenolic groups) (Alloway, 1995). Because this charge is pH dependent, the exchange capacity of organic matter diminishes with decreasing pH.

The CEC of a mineral soil is largely dependent upon texture; i.e., a clay soil will have a much greater CEC than does a sandy soil (Kingery et al., 2001). The type of clay also affects the CEC; i.e., 2:1 layer clays (such as smectites) have a greater CEC than 1:1 layer clays (such as kaolinite) (Miranda-Trevino and Coles, 2003). Organo-mineral complexes occur in soils as both metal (hydr) oxide and clay mineral associations, which act both to increase overall soil CEC and to play an important role in heavy metal-soil interactions (Petrovic et al., 1999; Kingery et al., 2001). Organic coatings enhance the exchange capacity of the soil by providing highly reactive organic functional groups and also increasing the effective surface area of the clay (Kingery et al., 2001). Although organic matter greatly increases the ability of soil colloids to adsorb metals through cation exchange, it is also well documented that Zn has a weak affinity for bonding with organics (Alloway, 1995; Manceau et al., 2000; Scheinost et al., 2002; Jacquat et al., 2009a).

## **2.2 Zinc speciation and fractionation in soils**

Zinc speciation is highly dependent on several factors that can both vary across the landscape and with depth at a single location (Roberts et al., 2002). Initially, Zn speciation depends on the input forms, for smelter sites these typically include primary Zn minerals (i.e., sphalerite or franklinite) and occasionally an oxidized zinc sulfate (Roberts et al., 2002). These particulates are aerially deposited, with the heaviest and largest particles found in high concentrations close to the contamination source (Yuan-Gen et al., 2009). Once these Zn particles are deposited into the soil environment, chemical speciation can be drastically altered depending on the chemical properties of the soil and climate (Jacquat et al., 2009a; Ciszewski et al., 2012; Liu et al., 2012). The dominant soil property influencing Zn speciation in the environment is pH, which significantly affects both the rate of primary Zn mineral weathering and the type of secondary Zn species that form after weathering occurs (Manceau et al., 2000; Jacquat et al., 2009a; Voegelin et al., 2011).



Soil contamination with Zn and other heavy metals is common, and Zn speciation has been performed on numerous contaminated sites throughout the world (Manceau et al., 2000; Roberts et al., 2002; Nachtegaal et al., 2005; Yuan-Gen et al., 2009; Sivry et al., 2010). Several recent studies of smelter contaminated soils used XAS and synchrotron techniques to provide new insights into how Zn reacts in the soil (Roberts et al., 2002; Jacquat et al., 2008; Sivry et al., 2010; Voegelin et al., 2011). Studies on soils contaminated with Zn have yielded information on the interactions of smelter released Zn with acidic soils under highly eroded landscape conditions that are quite similar to the area surrounding the smelter in Flin Flon. However, it was apparent after an extensive literature search that Zn speciation in sub-arctic climate and mixed wood Canadian boreal forest ecosystems has not been undertaken. In fact, the reactivity of Zn in boreal forest soils has been identified specifically as a research gap by Jacquat et al. (2009a).

Working with Zn smelter-affected soils in Palmerton, PA, Roberts et al. (2002) used both chemical extraction and synchrotron techniques to demonstrate potential phytotoxicity. They found that a large portion of Zn located in the surface horizon was non-labile, with only 13% of the total Zn being extractable. They also found, using EXAFS spectroscopy, that a large percentage of total Zn in the surface horizon was present as the Zn minerals franklinite ( $\text{ZnFe}_2\text{O}_4$ ) and sphalerite ( $\text{ZnS}$ ). In contrast, subsurface Zn speciation was dominated by Zn adsorbed to gibbsite (ca. 60%) and Zn in solution (ca. 40%). Roberts and coworkers reasoned that labile Zn is released as the non-soluble ore is slowly oxidized over time, and is subsequently transported into subsurface horizons by water percolating through the soil. While the total surface Zn concentration was much higher than was Zn concentration in the subsurface, the subsurface Zn was present in a more labile form that contributed to the toxic effects observed in the vegetation. This labile Zn was found to be weakly bound to the aluminum groups of clay particles, with a smaller percentage bound to manganese and iron (hydr) oxides. Even these Zn-metal oxide complexes remained available for plant uptake.

Nachtegaal et al. (2005) studied soils from a Zn contaminated site in Europe and found results similar to those of Roberts et al. (2002). Specifically, they found that a significant percentage (30–50%) of total Zn was present as the primary ore minerals, which depending on conditions, could weather into more labile secondary Zn species. A

greater percentage (50–70%) of the total Zn was determined to be previously weathered ore, with a high potential solubility. However, only 8% of the total Zn was able to desorb using calcium chloride [which was identical to the Roberts et al. (2002) study] suggesting that only a small percentage of total Zn is readily available (Nachtegaal et al., 2005). They also found that about 30% of the total Zn was desorbed when using an acidic nitric acid solution indicating that a much higher concentration of available Zn may occur in the rhizosphere as a result of the release of acidic root exudates. These results suggest that there may have been more plant available Zn in the soils studied by Roberts et al. (2002), which were also significantly more acidic than those studied by Nachtegaal et al. (2005). In contrast to the work of Roberts et al. (2002), Nachtegaal and co-workers (2005) found that, at neutral pH, secondary Zn occurred primarily in a Zn-Al layered double hydroxide (LDH) precipitate phase. Under acidic conditions (< pH 4), this Zn-Al-LDH was found to be unstable, releasing Zn into the soil solution. This re-release of Zn upon acidification of the soil may possibly explain why it was not observed in the acidic soils studied by Roberts et al. (2002). These studies demonstrate that Zn speciation is site-specific, requiring a detailed knowledge of the chemical properties of the soil.

A recent study by Voegelin et al. (2011) used soil artificially contaminated with sphalerite (ZnS) or zincite (ZnO), at a concentration of 2000 mg Zn kg<sup>-1</sup> soil, and ranging in pH from acidic (4.2) to slightly calcareous (7.7). They found that for all soil pH conditions zincite is more susceptible to weathering processes than is sphalerite (Voegelin et al., 2011). This study indicates that, in addition to secondary Zn species, Zn mineral dissolution rates are highly influenced by soil pH. At pH (4.2), zincite would undergo rapid chemical weathering to release Zn<sup>2+</sup>; in soils with near neutral pHs (7.7), the mineral is far more resistant to weathering processes. Sphalerite behaves differently, as it is more resistant to weathering under acidic conditions but, is more susceptible to weathering at neutral pHs following oxidative pathways (Voegelin et al., 2011). The soils in this study varied in pH from 4.2 to 7.7, allowing for the formation of several different secondary adsorption species and precipitates. In soils with a pH <5, the dissolution of zincite released Zn<sup>2+</sup> into the soil, which then formed predominantly octahedral inner- and outer-sphere adsorption complexes (~50% of total Zn). In these same acidic soils, the dominant precipitate was a Zn-Al hydroxy interlayer material (HIM). This precipitate decreased in

concentration with increased soil pH and was below detection limits in the soil with near neutral pH. They also found that HIM concentrations did not increase with time indicating that its formation is rapid in the soil and not time-dependent (Voegelin et al., 2011). As the soil pH increased, the total Zn bound as adsorption complexes decreased and transitioned to a Zn-Al-LDH precipitate. The adsorption species favoured at near neutral pH were generally tetrahedral inner-sphere complexes (i.e., Zn adsorbed to Fe oxides). The formation of an LDH precipitate is in agreement with studies completed by Roberts et al. (2002) and Nachtegaal et al. (2005) for soils near neutral pH. Voegelin et al. (2011) also reported that while Zn-Al-LDH formation was favoured in heavily contaminated soils, the combination of slow release of Zn from the weathering of minerals and the lower total concentrations in their artificially-spiked soils favoured the formation of adsorption species.

An important finding of the Voegelin et al. (2011) study was the stability of sphalerite in acidic soils with a pH of 4.2 and its subsequent dissolution at a near neutral pH of 7.7. Contrary, to Voegelin et al. a more theoretical based study of the dissolution rates of sphalerite completed by Acero et al. (2007) under acid mine drainage pH conditions (1-4.2) found that with sphalerite solubility increases with decreasing soil pH. The pH differences between studies is one likely determining factor the differences in solubility's as well as the potential differences in elemental composition of the two sphalerite minerals as they are from different sources.

Jacquat et al. (2009b) studied the release of Zn from the weathering of Zn-rich limestone minerals during soil formation to determine how Zn speciation was affected at neutral to alkaline pH. Unlike heavily contaminated anthropogenic soils, the Zn concentration from the dissolving limestone minerals was significantly lower, demonstrating the reactivity of soil minerals with  $\text{Zn}^{2+}$  in under saturated conditions. Aqueous  $\text{Zn}^{2+}$  in this study is a result of the weathering of Zn-rich limestone that also buffered the soil at alkaline pH. The initial Zn speciation in the limestone minerals was a mixture of either a Zn substituted calcite ( $\text{CaCO}_3$ ), sphalerite, or Zn sorbed to goethite. After contamination, the pedogenic Zn species that formed were adsorption complexes of Zn-goethite, Zn-kaolinite, and a Zn-Al-HIM precipitate (Jacquat et al., 2009b). Formation of the Zn-kaolinite fraction was the result of long-term weathering/transition of Zn-rich

smectites from the limestone to dioctahedral smectites with low Zn concentrations and finally into a very stable Zn-kaolinite fraction.

This Zn-kaolinite fraction had a low capacity for naturally attenuating large amounts of Zn, prompting Jacquat et al. (2009b) to theorize that uptake capacity was determined by the abundance of kaolinitic clays. In samples containing 25% kaolinite clay a maximum concentration of  $\sim 1000 \text{ mg Zn kg}^{-1}$  kaolinite was immobilized. Unlike the previously discussed studies of near neutral to alkaline soils, Jacquat and co-workers did not observe either Zn-Al-LDH or Zn-phyllosilicates, and the absence of these species was attributed to the combination of low Zn concentrations and a soil pH below that at which Zn-phyllosilicates typically form (Jacquat et al., 2009b). The long-term stability of the final Zn species was determined to be, in increasing order, Zn-Al-HIM < Zn-goethite < Zn-kaolinite.

A combined literature review of Zn contaminated sites and speciation study of Zn contamination from galvanized power lines by Jacquat et al. (2009a) examined the main factors effecting Zn fractionation in soils. They sought to understand Zn fractionation under a variety of pH and environmental conditions, with a focus on the formation of Zn precipitates and adsorption complexes. Soil pH ranged from 4.1 to 7.7, and Zn concentrations ranged from  $\sim 200 \text{ mg Zn kg}^{-1}$  to  $\sim 30,000 \text{ mg Zn kg}^{-1}$ . Adsorption complexes were classified as either tetrahedral or octahedral complexes, with octahedral coordination dominating at acidic pH (i.e., outer-sphere, Zn adsorbed with Mn oxides) (Jacquat et al., 2009a). At near neutral pH, Zn inner-sphere adsorption complexes were present in both tetrahedral and octahedral coordination. A strong pH effect also was seen with soil precipitates. The dominant soil precipitate was a Zn-Al-LDH soil precipitate; this phase formed across the widest range of contamination gradients (i.e., from  $\sim 1000$  to  $\sim 30,000 \text{ mg Zn kg}^{-1}$  soil) and across a pH range from 5.5 to 7.8. Zinc phyllosilicates were also found in neutral to slightly alkaline soils but did not account for a significant percentage of the Zn present (Jacquat et al., 2009). This indicated that Zn-Al-LDHs were the favoured precipitate at near neutral soil pH. In highly calcareous soils and at the highest Zn concentrations, precipitation of hydrozincite (Zn carbonate) minerals was dominant. At low Zn concentrations and under acidic conditions Zn-Al-HIM was the dominant precipitate (Jacquat et al., 2009a).

These studies collectively demonstrate several distinct trends affecting Zn fractionation that may also be occurring in the smelter-impacted soils of Flin Flon, MB. They also highlighted the major chemical characteristics and mechanisms that influence Zn speciation in soils, and the potential for phytotoxic effects. In the majority of contaminated acidic soils, Zn was initially present as the primary smelter produced minerals (franklinite, sphalerite and willemite) (Scheinost et al., 2002; Jacquat et al., 2009a; Voegelin et al., 2011). Upon the weathering of these minerals,  $\text{Zn}^{2+}$  was released and formed secondary adsorption and precipitate species. The chemical properties of the soil environment, specifically pH and total Zn concentration, both significantly influence Zn fractionation (Manceau et al., 2000; Voegelin et al., 2002; Jacquat et al., 2009a; Voegelin et al., 2011).

Under acidic conditions (pH 3.8 to 4.5) and with a sufficient supply of Zn and Al, the dominant precipitate is expected to be Zn-Al-HIM. It is stable and effectively lowers both Zn and Al phytotoxicity, though it is unable to form in heavily contaminated soils (Jacquat et al., 2009c). If the soil pH is increased to 6, Zn-Al-LDH precipitates may begin to form; for acidic soils these precipitates are unlikely to form without the addition of a liming agent (Nachtegaal et al., 2004; Jacquat et al., 2008). The extremely acidic nature of many smelter contaminated sites limits the formation of inner-sphere adsorption species (Voegelin et al., 2011). In acidic mineral soils, Zn adsorption typically occurs only with Si and Mn oxides as the low PZC allows them to be reactive at pHs >4, while Fe oxyhydroxides become reactive if the pH >5 (Nachtegaal and Sparks 2004; Feng et al., 2007; Jacquat et al., 2009a). Zinc adsorption to organics is rarely observed (Jacquat et al., 2009a); Zn-organic bonding was found only in organic soils at near neutral pH, indicating a lack of affinity for Zn to organic functional groups (Sarret et al., 2004).

### **2.3 X-ray Absorption Spectroscopy**

The use of X-ray absorption spectroscopy (XAS) as a tool for determining the speciation of contaminants in landscapes is an established practice in site assessment (Manceau et al., 2000; Sivry et al., 2010; Voegelin et al., 2011). The benefits of XAS based speciation reduce the reliance on operationally-defined extraction techniques for

determining speciation (Alloway, 1995; Manceau et al., 2000; Malandrino et al., 2011; Degryse et al., 2011; Baker et al., 2012; Churakov and Daehn, 2012).

### **2.3.1 X-ray absorption spectroscopy techniques**

The most common XAS techniques used for speciation in heavy metal contaminated soils are K-edge X-ray absorption near edge structure (XANES) and extended X-ray absorption fine structure (EXAFS) spectroscopies. The XAS methods probe the atomic structure and bonding environment of the element directly (Rehr and Albers, 2000; Yano and Yachandra, 2009). They differ in that XANES probes the area directly surrounding the absorption edge of an element, measuring changes in photon release intensity as the energy of the incoming beam increases over the absorption edge of the element (Eisenberger and Kincaid, 1978; Rehr and Albers, 2000; Yano and Yachandra, 2009). The EXAFS of an XAS scan provides chemical information about the atoms around the main element through the collection of constructive and destructive interference wave patterns generated by the release of photons from the element of interest (Eisenberger and Kincaid, 1978; Limpijumnon et al., 2006; Yano and Yachandra, 2009). The wave patterns generated by the backscattering atoms provide several chemical parameters that can be directly attributed to the speciation of the molecule (Rehr and Albers, 2000). In traditional EXAFS analysis of a single chemical species, the characteristic scattering patterns of the photoelectric wave can be modeled via shell by shell fitting using theoretical scattering paths. This analysis provides the coordination number, bond distances, and bonding geometries of neighbour atoms, and thus the short-range structure of the material can be derived from EXAFS (Rehr and Albers, 2000).

In more heterogeneous systems such as soils where multiple species of an element are present, the collected spectra represents the average local environment of all the species present, which complicates the traditional analysis technique of fitting a Fourier transformed spectra of EXAFS oscillations (Manceau et al., 2000). Instead, statistical analysis techniques such as Principal Component Analysis (PCA) and/or Linear Combination Fitting (LCF) are commonly used to de-convolute the relative contributions of each species from the heterogeneous XANES or EXAFS spectra (Jaquat et al., 2009a; Voegelin et al., 2011).

### 2.3.2 XAS Linear combination fitting

To be thorough, LCF requires a large database of potentially relevant Zn standards (Manceau et al., 2000; Voegelin et al., 2011). The number and relative amounts of the standard spectra are then systematically varied in software to create simulated mixtures until a model converges that best describes the experimental data (Voegelin et al., 2011). Although LCF is a powerful technique for determining the mixtures of different species in environmental systems and soils, it is not a stand-alone technique as there may be multiple combinations of standards that will result in acceptable fits of the experimental data. To improve confidence in LCF results, other chemical evidence is typically used in combination with XAS modeling. This supporting chemical data usually involves wet chemistry (soil pH,  $\text{CaCl}_2$  extractions, and total elemental analysis) and knowledge of the mechanisms responsible for Zn fractionation. The use of XANES LCF modeling can accurately determine species with large differences in bonding geometry/crystal structure (Yano and Yachandra, 2009) such as variations in oxidation state and coordination number. Linear combination fitting is less sensitive to picking out species with chemical similarities, such as adsorption complexes with the same coordination geometry (Manceau et al., 2000). Another limitation in LCF is that elements that are strong backscatters (i.e., Fe and Mn for soil samples) are preferentially included over lower molecular weight elements (i.e., Si and Al) (Manceau et al., 2000; Yano and Yachandra, 2009).

Linear combination fitting quantitatively determines the reference standards that collectively form to recreate the sample spectra. An example of bulk LCF EXAFS analysis is shown in Fig. 2.1. The LCF of EXAFS uses the constructive and destructive interference patterns of the standards to model, as closely as possible, the experimental spectrum of a sample. As previously noted, distinguishing among standards with similar bonding geometry is problematic due to similarities in the EXAFS pattern.

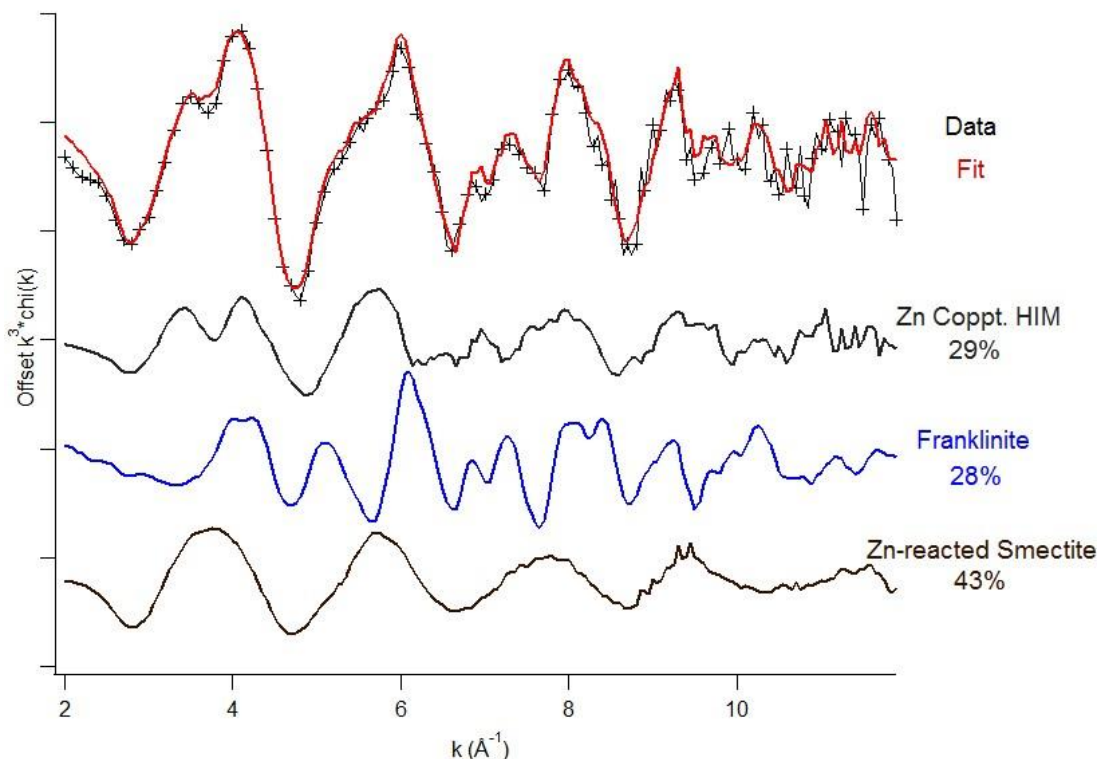


**Fig. 2.1.** Example of linear combination fitting (LCF) modeling of a bulk EXAFS soil sample from Flin Flon. Experimental data is shown in black with + symbols, the best fit LCF model is shown in red, and the 3 standard components (Zn-Al-HIM, franklinite, and Zn adsorbed on a smectite clay) and their relative proportions are shown below the fit.

### 2.3.3 X-ray microprobe ( $\mu$ XRF mapping and $\mu$ XANES)

One helpful technique for determining the validity of bulk XAS LCF is the use of spatially resolved X-ray microprobe techniques. X-ray fluorescence mapping ( $\mu$ XRF) can determine the spatial distribution of soil elements, especially metal contaminants (Roberts et al., 2002; Sarret et al., 2004; Nachtegaal et al., 2005). Typically, XRF image mapping and tri-colour plots are made using a high-energy micro-focused (spot sizes typically 1-10  $\mu\text{m}^2$ ) X-ray beam from a synchrotron to excite all elements with absorption edges below the incident energy (Manceau et al., 2000). The excited elements emit fluorescence at known emission lines that are measured by a fluorescence detector. Thus one can determine the concentration of each element from the measured intensity of the emission lines (Manceau et al., 2000).



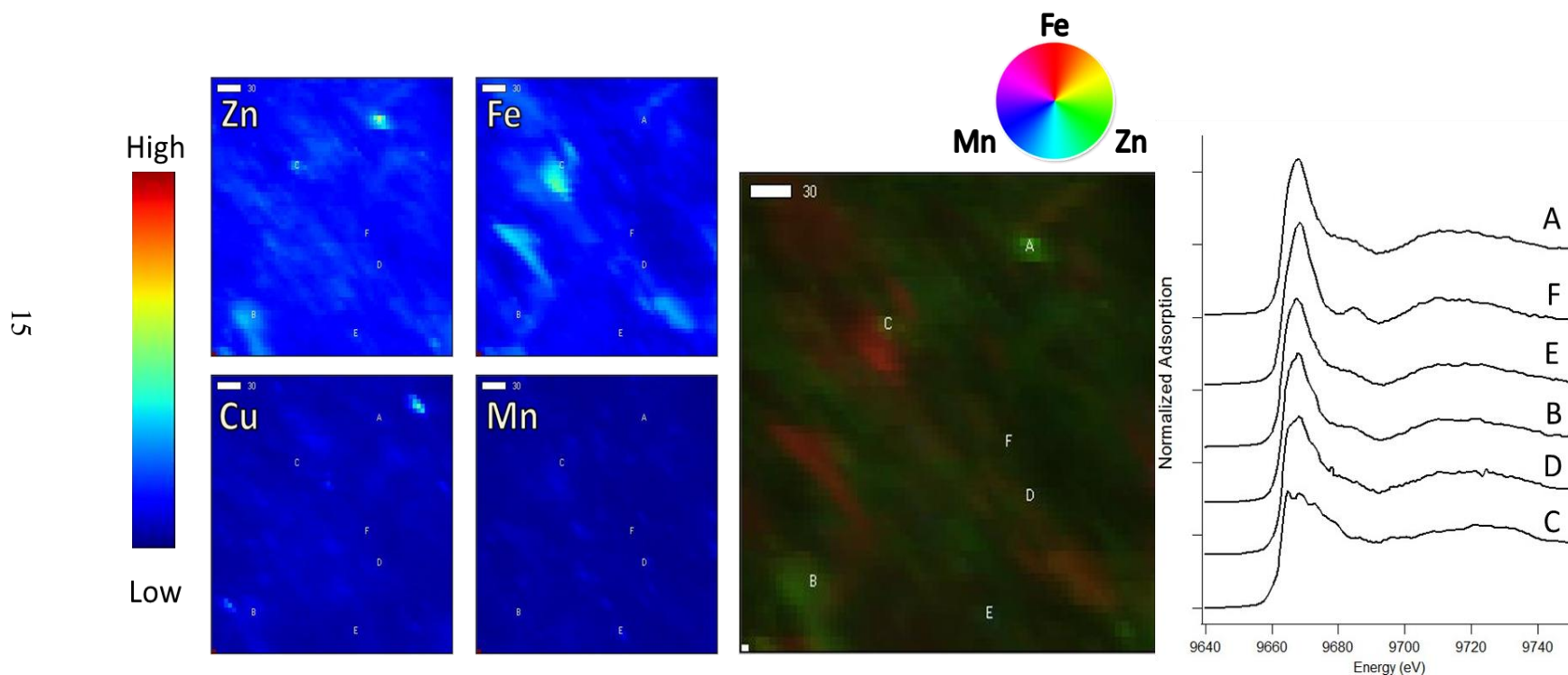


**Fig. 2.2.** Example results from an X-ray Microprobe experiment on a Flin Flon soil. (Left) X-ray fluorescence (XRF) intensity maps of Zn, Cu, Fe and Mn show the range of elemental concentrations in the sample. (Center) A tri-colour map of the XRF results indicating the relative concentrations of Zn, Fe and Mn and the co-location of these three elements. (Right) Zn K-edge  $\mu$ XANES spectra from interesting spots in the sample (labeled on the tri-colour map as (A-F) reveal differences in Zn speciation at the micro-scale.

The sample can then be rastered to obtain XRF at many points and produce spatially resolved 2D XRF maps. The relative fluorescence for all elements can then be converted to a color scale for every spot and plotted as a function of position to create elemental maps; convention is that lowest concentration is plotted as indigo while highest concentration is dark red. The resulting XRF map is highly useful to visualize relationships among elements in samples and thus is a complementary technique to combine with bulk or spatially resolved XAS speciation.

Interpreting XRF intensity maps, as displayed in Fig. 2.2, is based on the concentration of the element(s) of interest; each pixel in the map represents the concentration at that point in comparison to the highest concentration value within the image map, displayed as dark red. The areas of low concentration are dark blue, although the scaling is from the pixel of highest concentration. Thus a map with a single extremely high concentration point may diminish the intensity of all the other points towards what appears to be the background level. Since intensity maps are not scaled to the same reference concentration (i.e., Zn to Fe) they cannot readily be compared by concentration, only by collocation of elements. There is a large quantity of information within a single element's intensity map (i.e., Zn) that provides insight into the likely species present in the soil. For example, Zn maps showing a diffuse pattern throughout the entire sample may be indicative of secondary precipitates or adsorption species whereas discrete spots of high Zn intensity, commonly called hotspots, likely indicate the presence of primary mineral species (i.e., franklinite or sphalerite) in a sample.

### **3 ZINC SPECIATION IN A SMELTER AFFECTED BOREAL FOREST ECOSYSTEM: SITE CHARACTERIZATION USING EXAFS SPECTROSCOPY**

#### **3.1 Preface**

The phytotoxicity of heavy metals such as Zn cannot be elucidated by total concentration alone; detailed chemical speciation of the interactions occurring in soil environments is required to determine potential phytotoxicity. It has been previously determined that Zn is the limiting phytotoxic metal in the Flin Flon, MB smelter affected area, but provides no indication of the environmental mechanisms responsible for this phytotoxicity (Owojori and Siciliano, 2012). In this chapter (Chapter 3) Zn speciation was characterized using a combination of molecular-scale spectroscopic (XAS) techniques, chemical extractions, and soil pH. This chapter will provide the foundation of how Zn interacts in soils within the Flin Flon landscape and how it may be potentially altered to reduce this phytotoxicity. Speciation results will act as a baseline for expected speciation future chapters, when chronosequences of various ages will be studied to determine the effect of soil pH on Zn speciation in the Flin Flon landscape.

#### **3.2 Introduction**

Large-scale industrial mining and smelting activities have created hundreds of historically contaminated sites globally and have led to severe damage in many different ecosystems. The smelter area surrounding Flin Flon, MB is one such ecosystem, covering approximately 10,000 ha in the Canadian Shield. In addition to metal and acid deposition that is typical of smelter affected sites, a large percentage of the area has also experienced deforestation from several large forest fires and has been unable to recover naturally. Instead, many areas of the Flin Flon site have been colonized by metal tolerant grasses that outcompete the natural boreal forest vegetation. The major challenges at this site are high metal concentrations, particularly zinc and copper, and Al phytotoxicity resulting from acid deposition as a byproduct of smelting sulphide ores (Henderson et al., 1998;

McMartin et al., 1999; Scheinost et al., 2002). The speciation, rather than total concentration of an element often correlates to toxicity in contaminated soil environments (Basta et al., 2005; Voegelin et al., 2011). Accordingly, reclaiming these ecosystems requires characterization of not only the extent of heavy metal contamination but also the detailed chemical speciation of the phytotoxic metals (Scheinost et al., 2002). X-ray absorption spectroscopy (XAS) at the Zn K-edge is a powerful molecular-scale tool for obtaining detailed Zn speciation data in contaminated soils. Detailed XAS-based chemical speciation of Zn in contaminated soils has been characterized in a range of soil environments with differing Zn input sources, soil properties, site histories, and pedogenic processes (Manceau et al., 2000; Scheinost et al., 2002; Nachtegaal et al., 2005; Jacquat et al., 2009a; Degryse et al., 2011).

At the majority of Zn smelter contaminated sites, Zn is initially released into the environment as a combination of the primary minerals franklinite, sphalerite and willemite (Jacquat et al., 2009a). Franklinite ( $\text{ZnFe}_2\text{O}_4$ ) is a Zn-Fe spinel mineral, which occurs naturally and forms at high temperatures during smelting of Fe-rich ores (Alloway, 1995; Scheinost et al., 2002; Roberts et al., 2002). Franklinite weathers slowly in most natural environments and persists for decades while slowly releasing  $\text{Zn}^{2+}$  into the soil (Alloway, 1995). Sphalerite ( $\text{ZnS}$ ) is a reduced sulphide mineral that also forms at high temperatures during smelting (Scheinost et al., 2002; Voegelin et al., 2011), but may be more susceptible to biogeochemical weathering in soils to release  $\text{Zn}^{2+}$  (Scheinost et al., 2002; Voegelin et al., 2011). Willemite ( $\text{Zn}_2\text{SiO}_4$ ) is typically a minor component of naturally occurring franklinite and sphalerite ore bodies (Alloway, 1995). In the sub-arctic climate characteristic of the Flin Flon, MB site, the chemical weathering rates of these minerals may be slow due to low temperatures, which could allow them to persist much longer in the environment than in warmer climates.

Aqueous Zn released from the weathering of Zn minerals is known to form several secondary phases depending upon pedogenic processes and characteristics of the soil (Manceau et al., 2000; Scheinost et al., 2002; Van Damme et al., 2010; Voegelin et al., 2011). Chemical controls on Zn speciation include pH, Zn concentration, and soil mineralogy (Pokrovsky et al., 2005; Jacquat et al., 2009a). In acidic soils typical of the smelter-affected Canadian shield, rapid and highly reversible adsorption of Zn as outer-

sphere complexes on the exchange sites of permanently-charged phyllosilicates and inner-sphere surface complexes with low point of zero charge (PZC) minerals (Si and Mn oxides) are known to occur (Tschapek et al., 1974; Voegelin et al., 2002; Feng et al., 2007; Jacquat et al., 2009a; Kwon et al., 2013). Soil precipitates such as Zn-Al-hydroxy interlayer material (HIM) can form as a co-precipitate or as an adsorption complex in acidic soils (Scheinost et al., 2002; Jacquat et al., 2009c). The formation of Zn-Al-HIM can reduce the phytotoxicity of both Zn and Al, and typically forms in contaminated soils with Zn concentrations less than 2000 mg kg<sup>-1</sup> and at soil pHs between 4 and 4.5 (Scheinost et al., 2002; Jacquat et al., 2009c). Near neutral soil pH, inner-sphere adsorption complexes with Fe and Mn oxides become significantly more stable and less susceptible to desorption (Nachetgaal and Sparks, 2004; Nachetgaal et al., 2005). The dominant Zn precipitate that forms under slightly acidic to neutral pH and oxic conditions is a Zn-Al-layered double hydroxide (LDH) (Roberts et al., 2003; Voegelin et al., 2011). This stable precipitate is commonly found in both calcareous and slightly acidic (pH 6) soils contaminated with Zn. The formation of Zn-Al-LDH reduces long-term Zn phytotoxicity, as it remains stable even under acidic or high ionic strength soil solution conditions (Voegelin et al., 2011).

Since there is widely different stability and toxicity associated with these different Zn species, characterizing Zn chemistry throughout the affected landscape is an important step in reclaiming this affected region and making informed recommendations to revegetation efforts. The objectives of this study were to: (1) characterize the dominant forms of Zn in smelter-impacted boreal forest soil from of Flin Flon, MB and (2) evaluate the links between landscape position, onsite vegetation and Zn speciation in these soils.

### **3.3 Materials and Methods**

#### **3.3.1 Soils**

Soils were collected from seven sites (Fig. 3.1) in the vicinity of the HudBay Minerals smelter located at Flin Flon, MB. These sites are separated by (a) direction and distance from the processing facility, (b) slope position, (c) vegetative cover, and (d) soil chemical properties. These features influence both Zn concentration and chemical speciation; notably the sites downwind (North and East) of the smelter typically have significantly

higher Zn concentrations than those located south of the smelter. The seven sites chosen encompass a range of topography and soil structure, but can largely be classified into two groups. Sites 3, 5, 6, 7 have zero to minimal plant cover and occur in upper or mid slope convex positions, thus they are susceptible (i.e. Fig. 3.1, Site 3 photo) to wind and water erosion. Soils from these sites were sampled from different slope positions with one site (Site 5) located at the pinnacle of an eroding rock outcrop, were in mid-slope positions (Sites 3 and 6), and the last was from a low-slope position (Site 7). Sites 1, 2, and 4 are located in more stable areas, having been colonized by a metal tolerant grass species, and are typically level with concave features or depressions (Fig. 3.1, Site 2). Soil stability facilitates soil development and the accumulation of organic matter from the metal tolerant plants. Zinc speciation was examined in both the surface 0-2 cm of soils and at a subsurface depth of 8-10 cm to characterize the dynamics of Zn speciation in the rooting zone of the established vegetation.

### **3.3.2 Soil analysis**

Soil pH was measured in 0.01 M  $\text{CaCl}_2$  with a solution-soil ratio of 10:1(w/v) (Nachtegaal et al., 2005; Jacquat et al., 2009a). The soil and  $\text{CaCl}_2$  solution were thoroughly mixed for 30 min and then allowed to settle for 2 h before measurement (Nachtegaal et al., 2005; Jacquat et al., 2009a). Plant available metals were determined by batch replenishment extractions using 10 g  $\text{L}^{-1}$  suspensions of soil in 0.1 M  $\text{CaCl}_2$  adjusted to pH 4.5 with 0.1 M nitric acid (Strawn and Sparks, 2000; Nachtegaal et al., 2005). A filter flow extraction technique (Eick et al., 1999; Roberts et al., 2002) was used to determine that the 10 g  $\text{L}^{-1}$  suspension density desorbed the entirety of Ca-exchangeable Zn. The extraction procedure consisted of three replenishments of 35 mL extracting solution shaken at 100 RPM; they were filtered (using 0.2  $\mu\text{m}$  filters) and replenished every 24 h. The filtrate was then diluted (as needed) for analysis using an Agilent 4100 microwave plasma atomic emission spectrometer (MP-AES) Agilent Technologies; Mississauga, ON). Total elemental concentrations were determined via microwave digestion with EPA method 3051; this required 9 mL of 37% HCl and 3 mL of 65%  $\text{HNO}_3$  for a total volume of 12 mL per 0.5 gram of soil (Chen and Ma, 1998). The digested solution was then filtered with a 0.2  $\mu\text{m}$  filter and diluted for analysis using an Agilent 4100 MP-AES [Agilent Technologies (Mississauga, ON)].

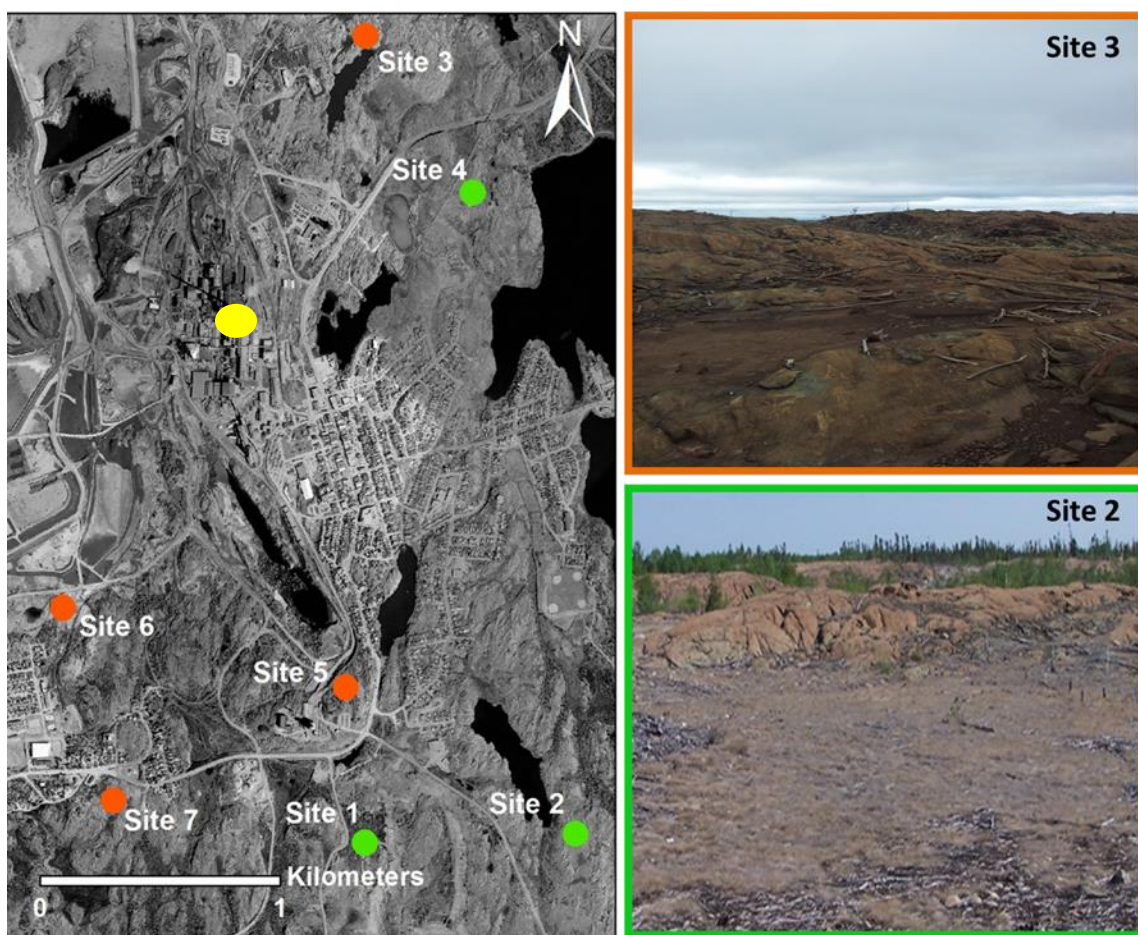


**Fig. 3.1. Sampling sites used in characterizing Zn speciation in relation to the smelter/processing facility (Yellow). High erodibility (Orange) and stabilized (Green) soils are indicated with picture representations defining each classification. Aerial photo provided by University of Saskatchewan Department of Soil Science Soil Survey of Flin Flon, MB.**

### 3.3.3 XAS data collection and analysis

All XAS measurements were conducted at the Canadian Light Source (CLS) synchrotron in Saskatoon, SK. The CLS storage ring operates at 2.9 GeV and 250-150 mA. Bulk (0.1-0.5x0.1-0.5mm spot size) XAS measurements were collected at the CLS's HXMA beamline (06ID-1). An extensive library of Zn standards were collected, and the methodology used to produce the standards as well as both the XANES and EXAFS spectra are compiled in Supplemental Information 1. All data was collected at the Zn K-edge (9659 eV) with a Si-220 monochromator detuned by 50% to suppress higher order harmonics. The monochromator was calibrated to the first inflection point of the K-edge Zn reference foil of 9659 eV; this Zn reference was simultaneously collected with each sample throughout the experiment. Concentrated Zn references were collected in transmission mode to eliminate self-absorption effects; transmission samples were diluted to ensure an edge step of between 1.5 and 2. Dilute Zn-reacted reference compounds and all soil samples were measured in fluorescence mode with a 32-element Ge detector (Canberra) and both a Cu-6 filter and Soller slits between the sample and detector to reduce scattering and unwanted fluorescence from other elements. When necessary, Al foil was also placed over the 32-element detector to improve signal to noise by preferentially reducing Fe fluorescence from samples.

With an extensive and detailed library of standard spectra, linear combination fitting (LCF) were used to de-convolute the different Zn species and their relative contributions to the Zn spectrum (Manceau et al., 2000; Jacquat et al., 2009b; Voegelin et al., 2011). To assist in choosing the correct LCF modeling strategy,  $\text{CaCl}_2$  extraction measurements, soil pH values, and other soil chemical properties can be incorporated into the analysis (Roberts et al., 2002; Voegelin et al., 2011).

X-ray fluorescence (XRF) maps were collected at the CLS VESPERS beamline (07B2-1). Mapping was completed using a "pink" beam at 20 keV capable of exciting all elements from K to As. X-ray fluorescence maps were collected with a four-element Vortex detector using a  $5 \times 5 \mu\text{m}$  spot size with a  $5 \mu\text{m}$  step size, with a one second integration time per data point. X-ray fluorescence maps of the soils ranged in size from  $300 \times 300 \mu\text{m}$  to  $500 \times 500 \mu\text{m}$ .



X-ray absorption spectroscopy data processing and analysis was performed using a variety of software. For bulk EXAFS data, ATHENA software was used (Ravel and Newville, 2005). Data reduction in Athena included processing, which included background removal, calibration, alignment and merging of individual scans. Bulk EXAFS data were then extracted using a  $k^3$ -weighted chi data over a range of 2-12  $k$  ( $\text{\AA}^{-1}$ ) after background subtraction and spline fitting, and Linear Combination Fitting (LCF) was then performed on all XANES and EXAFS data using a fitting range dependent upon data quality, typically 2-12  $k$  ( $\text{\AA}^{-1}$ ) (Ravel and Newville, 2005). For information regarding the criteria using in determining the LCF results or Zn reference spectra, see Appendix A. XRF mapping data reduction and analysis was done using SMAK software (Sam Webb, SSRL) to normalize and then generate element specific intensity and tri-colour maps.

### **3.4 Results and Discussion**

#### **3.4.1 XRF image maps and contaminant spatial distribution**

Two soils, one each from Sites 4 and 7 (Fig. 3.1) were selected for XRF mapping, these soils were representative of the erodible and stabilized classifications. See Chapter 2, Section 2.3 for additional information on interpreting XRF intensity and tri-colour maps. The soil from Site 4 is a highly Zn contaminated soil with a metal tolerant grass vegetative cover that has reduced the potential for erosion. Soil from Site 7 (Fig. 3.1) is from a high erodibility landscape position that has experienced limited soil development and a reduced soil profile thickness.

The X-ray fluorescence (XRF) intensity and tri-colour map of the Site 4 surface soil (Fig. 3.2) indicate the spatial distribution of Zn with soil Fe and Mn within this subsample (500 x 500  $\mu\text{m}$  total size). Iron and Mn are two major soil components that have a high affinity with Zn and represent two possible reactive surfaces that Zn may be interacting with in the soil environment (Voegelin et al., 2002). The Zn intensity map and relative contributions of Zn in comparison to Fe and Mn in the tricolour plot illustrate the high level of Zn contamination in this soil (23,000  $\text{mg kg}^{-1}$  total Zn). Although there are areas of the tri-color map (represented in orange) that show Zn-Fe correlation, there is little direct association between Zn and soil Fe or Mn.

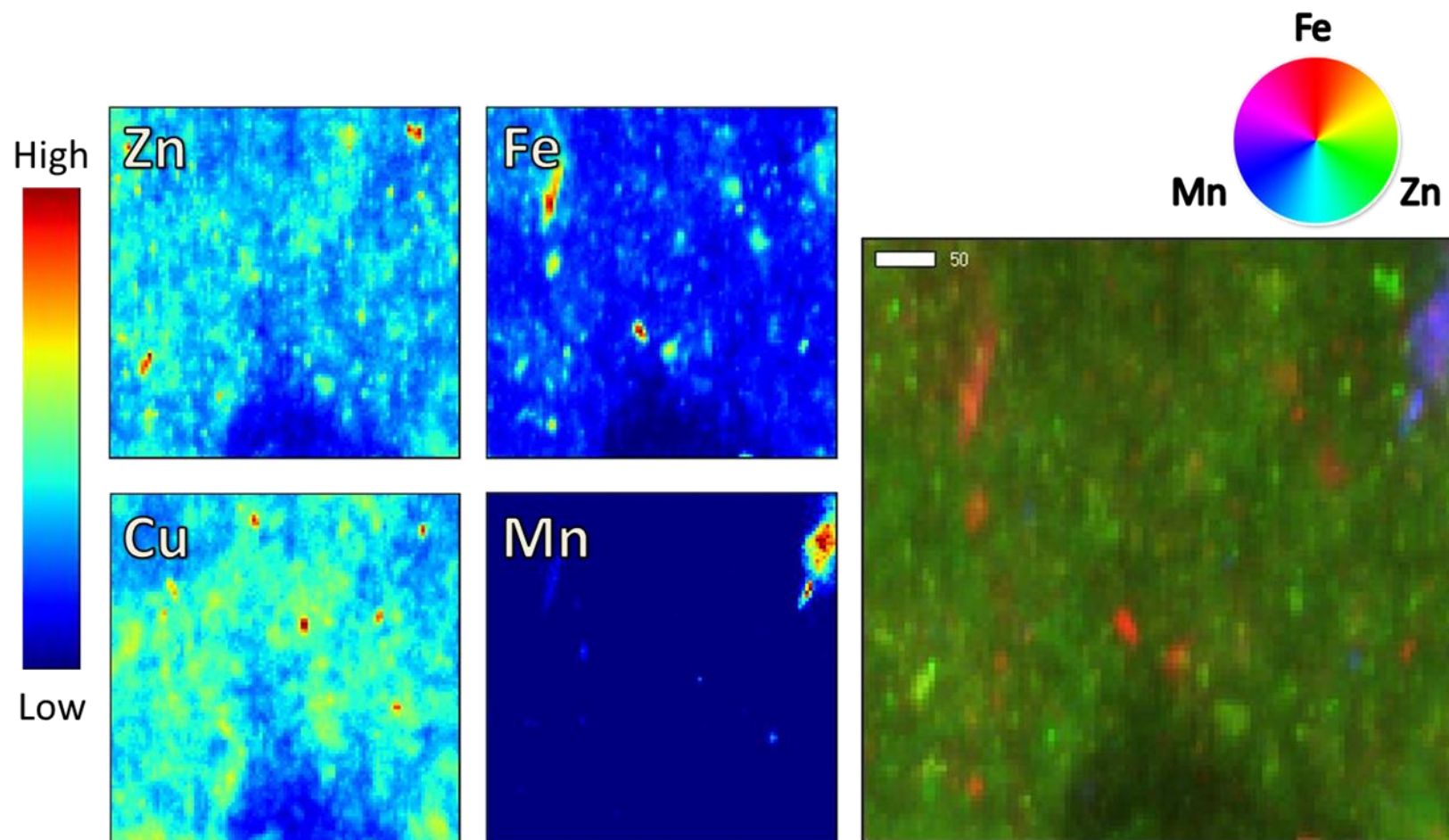


**Fig. 3.2.** Site 4 surface soil (0-2 cm) synchrotron XRF microprobe maps for Zn, Fe, Cu, and Mn. Colors denote intensity (red = relative high elemental concentration, dark blue = low relative elemental concentration) and tri-colour maps ( $500 \times 500 \mu\text{m}$ ) reveal 2D spatial relationships of Zn, Fe, and Mn throughout the soil.

The most likely Zn-Fe species, given a smelter as the source, are franklinite and Zn sorbed to iron oxides (Alloway, 1995; Roberts et al., 2002). However, the low pH of the soil (4.38) makes adsorption of Zn on Fe oxides unlikely (Nachtegaal et al., 2005). The relatively small size of the Zn hotspots and widespread distribution throughout the soil suggests that the quantity of large sphalerite or franklinite particles in the soil is small. Soil Mn appears to be present as concentrated large particles more so than do other elements.

The elemental distribution in the Site 7 surface soil (Fig. 3.3) is different from that of the Site 4 surface soil in Fig. 3.2. The Zn intensity map indicates that Zn is present primarily in discrete particles (Zn hotspots) that are not strongly correlated with Fe, and may be indicative of the primary smelter released minerals. The much lower overall Zn concentration in this soil compared to Site 4 is consistent with a soil experiencing high rates of erosion. As the smelter-deposited minerals weather, the released  $\text{Zn}^{2+}$  will leach downslope in high moisture conditions, thus limiting the formation of secondary Zn-Fe or Zn-Mn sorption/precipitation associations that retain Zn. There are some Zn and Fe correlations that are masked by the high Zn intensity in the remaining hotspots; this is again consistent with franklinite and not Zn sorption with Fe oxides, given the soil's acidic pH of 3.87 (Nachtegaal and Sparks, 2004). This may also potentially be indicating sphalerite particles that contain amounts of Fe from the smelter process.

### **3.4.2 Bulk Zn XAS speciation**

Bulk XANES (X-ray absorption near edge structure) and EXAFS (extended X-ray absorption fine structure) spectra of the soils (Fig. 3.4) show varied Zn speciation throughout the Flin Flon site. The raw XAFS spectra demonstrate the variation in Zn speciation between surface (0-2 cm) and subsurface soils (8-10 cm). Surface soils, regardless of location relative to the smelter, all have a significant component of franklinite. This can readily be observed in both the distinctive XANES fingerprint of three distinctive peaks through the absorption edge, and a characteristic EXAFS signal due to high frequency oscillations arising from strong X-ray backscattering of Fe. Several surface soils (Sites 1 and 2) also appear to have secondary Zn species based on XAS. This observation can be based on indicators in XANES spectra including changes in triplet peak shape and height intensity (especially a

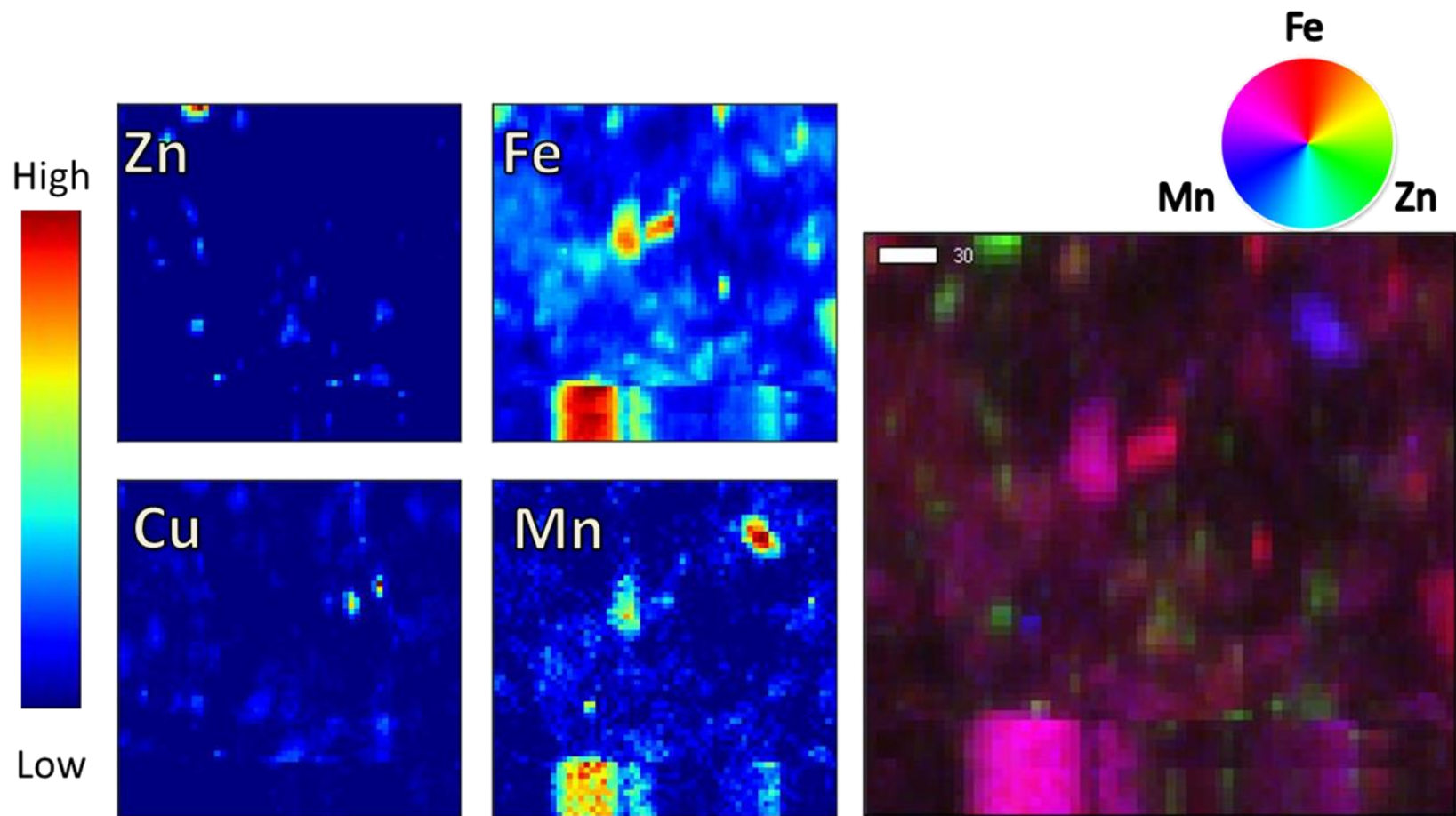


**Fig. 3.3.** Site 7 surface soil (0-2 cm) synchrotron XRF microprobe maps for Zn, Fe, Cu, and Mn. Colors denote intensity (red = high relative elemental concentration, dark blue = low relative elemental concentration) and tri-colour maps ( $300 \times 300 \mu\text{m}$ ) reveal 2D spatial relationships of Zn, Fe, and Mn throughout the soil.

dampening of the third peak). The EXAFS of these surface soils contain the distinct franklinite spectra; the secondary components have weaker contributions and contribute to dampening of the franklinite spectral EXAFS oscillations due to constructive and destructive interferences. Due to much lower Zn concentrations in the subsurface soils, XAS measurements were limited to XANES. In the subsurface, Zn was present as mixtures of either secondary phases (adsorption complexes and neo-phase precipitates) with some franklinite and sphalerite also present. Linear combination fits of the experimental XAS data can be found in Fig. 3.4, the results of the LCF model are compiled in Table 3.1, along with total and extractable metal concentrations, and erosional classification.

The major Zn components were similar for all soils; the major changes in speciation were differences in the relative abundance of each species. The dominant Zn species is franklinite, which must be resistant to physical and chemical weathering in this landscape to persist in high relative abundances over decades. Sphalerite is also observed in some soils, but at a lower relative abundance and reduced distribution. This suggests that sphalerite is more susceptible to weathering in this environment. Sphalerite has shown to be susceptible to dissolution at acidic soil pHs and thus is rationed to be the reason why it is only present in lower sloped positions (Acero et al., 2007).

The common Zn species found in all but two of the soils is an octahedral Zn species without any strong backscattering atoms that could add structure to the EXAFS. This species is consistent with the outer-sphere Zn reference standard (aqueous  $\text{Zn}^{2+}$ ). This Zn species is expected to be the most susceptible to desorption/extraction when environmental conditions (pH, ionic strength) change.

The translocation of outer-sphere and/or aqueous  $\text{Zn}^{2+}$  typically results in the formation of three secondary Zn species in the subsurface soils: Zn inner-sphere adsorption complexes with Mn oxides, Si oxides, and as a Zn-Al-hydroxy interlayer material (HIM) soil precipitate. The lower Zn concentration in the subsurface soils (Table 1) may lead to a higher relative abundance of adsorbed or neo-phase Zn species, or they may be minor components that are present in the higher concentration soils but below the detection limits of XAS (Jacquat et al., 2009c). The outer-sphere labile Zn fraction is the species most

likely to convert to these inner-sphere adsorption complexes as pH and reaction time increases (Manceau et al., 2000; Scheinost et al., 2002; Vespa et al., 2010).

The point of zero charge (PZC) and high Zn reactivity of Mn oxides enables adsorption to occur under the acidic conditions of these soils; this adsorption complex is expected to help immobilize Zn from the soil solution and may reduce phytotoxicity (Feng et al., 2007). Only two of the studied soils (Site 6 surface and subsurface) had a significant fraction of Zn adsorbed to Mn oxides, with a loading estimated of approximately 1000 and 400 mg Zn kg<sup>-1</sup> in the surface and subsurface soils, respectively. The CaCl<sub>2</sub> extractions indicate that this species was stable and thus less phytotoxic than the outer-sphere Zn fraction. In the remaining subsurface soils, the low Zn concentrations may have inflated the importance of the relative abundance of Zn sorbed to Mn oxides. Zinc adsorption to soil Si oxides was a significant component in several soils, including the most heavily Zn contaminated soil (Site 4). Formation of this inner-sphere adsorption complex reflects the combination of low PZC of SiO<sub>2</sub> and low reactivity of other adsorbents for Zn at low pHs (Tschapek et al., 1974).

The other secondary Zn phase, found only in the subsurface, is a neo-phase Zn-Al hydroxyl interlayer material (HIM). This co-precipitate forms when Zn<sup>2+</sup>, Al<sup>3+</sup>, and smectite clay sorbents are all available at a soil pH of between 4 and 4.5 (Scheinost et al., 2002). Zinc-Al-HIM typically forms when Zn soil concentrations are below 2000 mg Zn kg<sup>-1</sup> (Scheinost et al., 2002; Jacquat et al., 2009c). Zinc-Al-HIM is a stable species under acidic conditions and is resistant to CaCl<sub>2</sub> extraction (Table 1). This species may represent a likely natural attenuation mechanism that can simultaneously reduce the phytotoxicity of Zn and Al in the Flin Flon landscape.

### **3.4.3 Influence of soil erosion and slope position on Zn speciation**

X-ray absorption spectroscopy results suggest that the pedogenic processes of soil erosion are important to metal speciation in this landscape. Soils sampled from the seven sites can be separated based on field observations and the relative abundances of the different Zn species, specifically changes in the franklinite and aqueous Zn contributions, into two distinct designations (1) high erodibility/eroding soils, and (2) vegetative stabilized soils. The speciation within each class was found to be nearly identical, lending

confidence in scaling our speciation results to the broader Flin Flon site in general. Susceptibility to erosion and slope position are strong influences on Zn speciation because (1) of the accumulation of Zn in low slope positions, specifically the highly labile aqueous Zn fraction, and (2) increasing the relative abundances of the smelter-deposited minerals. The limitations of mineral weathering and potential adsorption/precipitation reactions are defined by the susceptibility (high or low) to soil erosion.

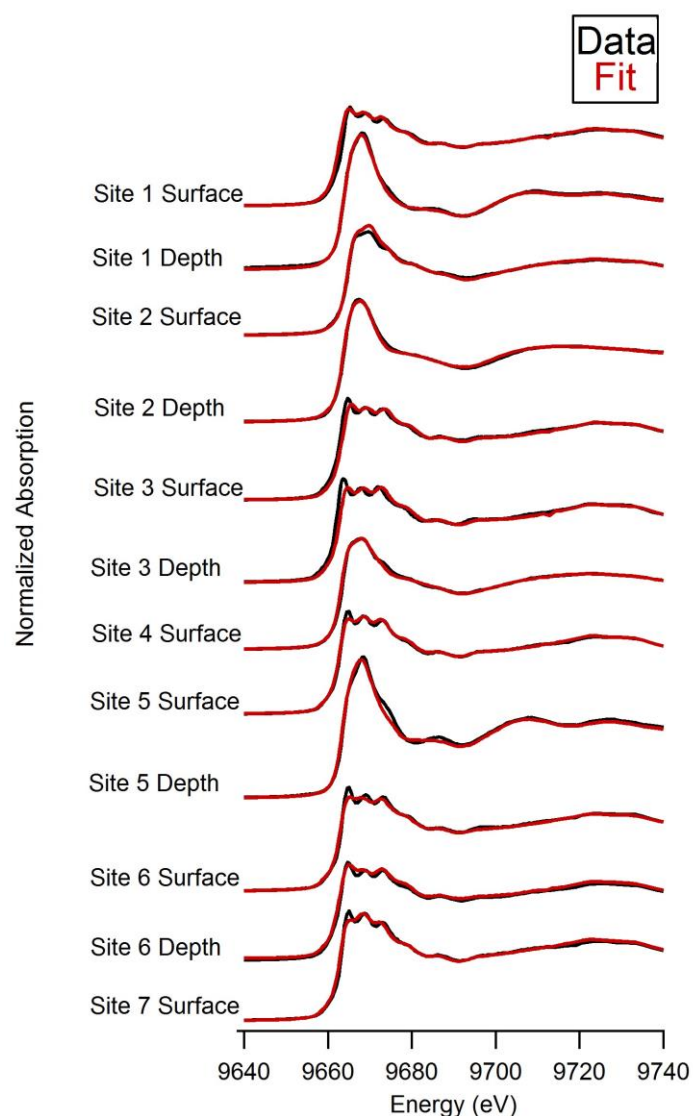


**Fig. 3.4. Bulk Zn K-edge XANES (black lines) with LCF model fits (red lines) of surface (0-2 cm) and subsurface (8-10 cm) measurements of studied sites surrounding the Flin Flon, MB smelter.**



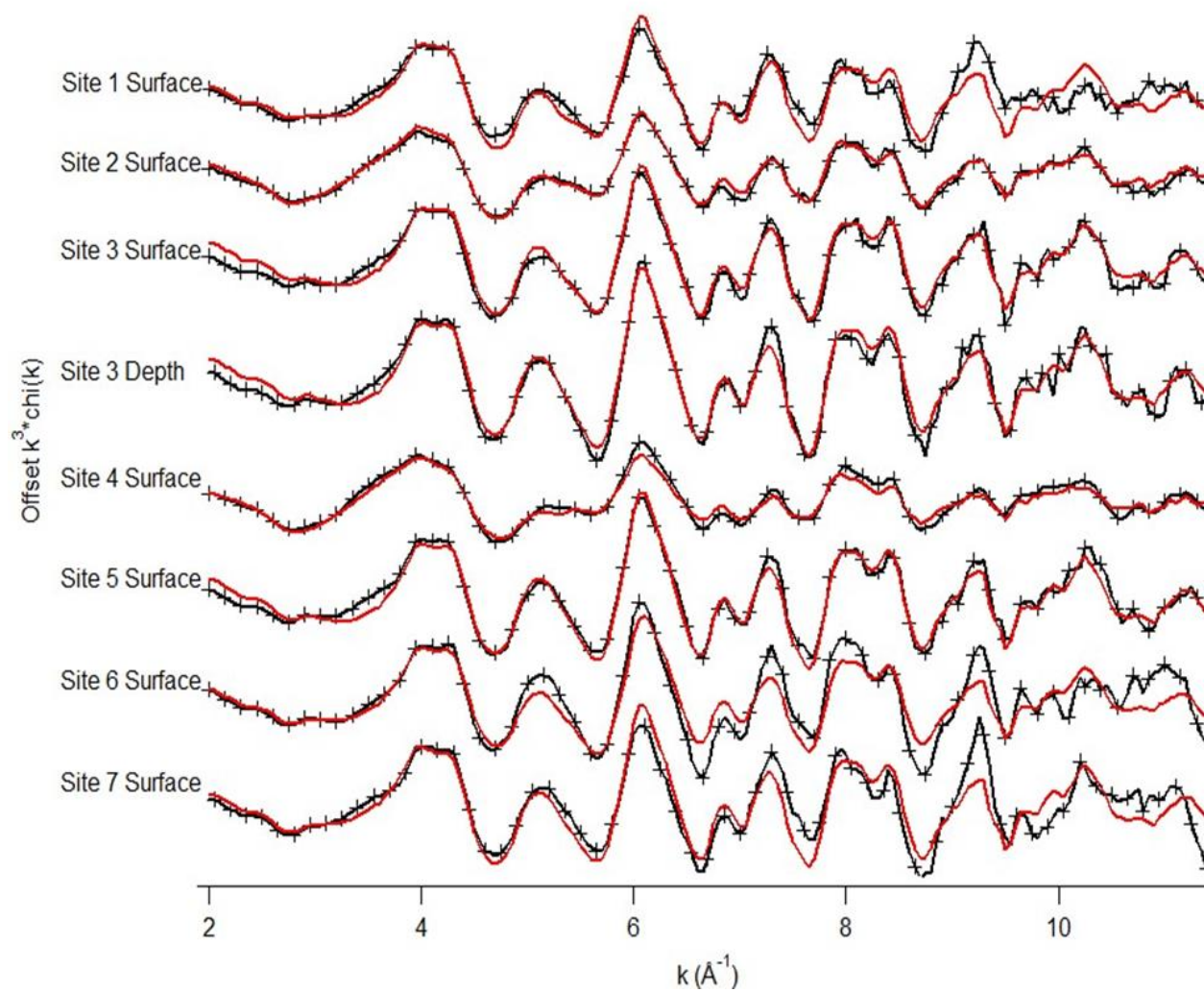


**Fig. 3.5. Bulk EXAFS with LCF model fits of surface (0-2 cm) and subsurface (8-10 cm) measurements of studied sites surrounding the Flin Flon, MB smelter.**



**Table 3.1. Bulk soil chemical analysis and XAS Linear Combination Fit (LCF)<sup>†</sup> results for surface (0-2 cm) and subsurface (8-10 cm) soils.**

Site ID	Slope Position	Depth	Vegetative coverage <sup>‡</sup>	pH	Total Digestible <sup>§</sup>	CaCl <sub>2</sub> Extractable <sup>¶</sup>		Franklinite (ZnFe <sub>2</sub> O <sub>4</sub> )	Sphalerite (ZnS)	Zn-Sorbed				Reduced Chi <sup>2</sup>
					Zn	Zn	Al			SiO <sub>2</sub>	MnO <sub>2</sub>	Outer-sphere/Aq. Zn	HIM	
		cm			mg kg <sup>-1</sup> soil					% <sup>#</sup>			Fit space <sup>††or ‡‡</sup>	
1	No-slope convex	0-2	+	3.5 ± 0.1	7219	1058	524	65	18	-	-	17	-	0.15 <sup>‡‡</sup>
		8-10		3.9 ± 0.1	175	70	156	-	-	-	20	44	36	3×10 <sup>-4††</sup>
2	No-slope concave	0-2	++	3.3 ± 0.1	10013 ± 155	9740	276	45	-	14	-	42	-	0.24 <sup>‡‡</sup>
		8-10		3.3 ± 0.1	604	534 ± 48	466 ± 36	-	-	21	24	55	-	3×10 <sup>-4††</sup>
3	Mid convex	0-2	-	3.8 ± 0.1	8865	651	470	77	11	-	-	12	-	0.31 <sup>‡‡</sup>
		8-10		3.8 ± 0.1	5485	287	1039	90	-	-	-	10	-	1.2 <sup>‡‡</sup>
4	Mid concave	0-2	+++	4.3 ± 0.1	23373 ± 2165	15740	180	28	-	29	-	43	-	0.39 <sup>‡‡</sup>
5	Upper convex	0-2		3.8 ± 0.1	1635	76 ± 5	242 ± 23	85	-	-	-	15	-	3×10 <sup>-4††</sup>
		8-10	4.2 ± 0.1	170 ± 15	47 ± 15	265 ± 28	-	-	-	-	23	77	1×10 <sup>-3††</sup>	
6	Mid convex	0-2	-	3.2 ± 0.1	5111	651	1640	62	18	-	20	-	-	0.43 <sup>‡‡</sup>
		8-10		3.2 ± 0.1	2062	38	746	65	-	13	22	-	-	2×10 <sup>-4††</sup>
7	Low convex	0-2	-	3.5 ± 0.1	1409	55 ±5	228 ± 24	79	-	-	-	21	-	7×10 <sup>-4††</sup>

<sup>†</sup> Eo Shift constrained to zero

<sup>‡</sup> Percent metal tolerant grass vegetation cover: (-) zero coverage, (+) 0-20%, (++) 20-40%, (+++) 40-60%

<sup>§</sup> Via total elemental digest

<sup>¶</sup> pH 4.5 CaCl<sub>2</sub> extractable

<sup>#</sup> % Relative contribution to XAS signal; models constrained to 100%

<sup>††</sup> Linear combination fit model of XANES data -20 to +100eV from the absorption edge (9569 eV)

<sup>‡‡</sup> Linear combination fit model of EXAFS data 2-12k (Å<sup>-1</sup>)

Sites where soil was physically stabilized by metal tolerant grasses have limited erosional losses and thus typically have higher Zn concentrations. These areas are largely level or depressional areas, and influxes of soil from the nearby eroding landscape help to buffer against acidification. Zinc speciation in the surface soils of these sites typically consists of franklinite (~50%); the stability of these soils has facilitated chemical weathering and lower relative abundance of this mineral species. The remaining Zn in these surface soils is a mixture of inner-sphere adsorption complexes with MnO<sub>2</sub> or SiO<sub>2</sub> sorbents and outer-sphere Zn adsorption complexes. The effect of soil stabilization is demonstrated in the increased relative abundance of adsorption species, the reactive soil surfaces forming these adsorption species would likely be preferentially redistributed in the landscape if soil redistribution was occurring. As well, if these surface soils were experiencing high rates of erosion and contaminant transport there would be little labile Zn present as it be transported elsewhere in the landscape/soil profile.

The stabilized subsurface soils also show signs of in-place soil development rather than being simply deposited/buried soil. As the presence of large relative abundances of secondary adsorption/precipitate species and low total (<~600 mg Zn kg<sup>-1</sup> soil) Zn concentrations are indicating that Zn is leaching through the soil profile and is not being deposited over previously deposited soil. Zinc movement in these soils is limited to transport through the soil profile via leaching; subsurface soils typically contain an order of magnitude less Zn than do the surface soils from the same site. The movement of labile Zn through the soil profile accounts for the changes in Zn subsurface soil speciation; nearly half the total Zn is present as outer-sphere adsorption complexes and the remaining fractions are inner-sphere adsorbed Zn on either soil Si or Mn oxides with no mineral species fraction present. This is consistent with Zn speciation that has been observed in the subsurface of other smelter-affected soils (Roberts et al., 2003; Nachtegaal et al., 2005; Feng et al., 2007; Voegelin et al., 2011). The formation of Zn-Al-HIM in the subsurface soil from Site 1 is evidence of natural attenuation of Zn (Scheinost et al., 2002; Jacquat et al., 2009c;), but Zn-Al-HIM formation in these subsurface soils may be limited by soil pH and Al<sup>3+</sup> availability (Jacquat et al., 2009a). The growth of metal-tolerant grasses on these stabilized soils increases soil organic matter, which in turn complexes Al and reduces Zn-Al-HIM formation (Alvarez et al., 2011; Collignon et al., 2012). The secondary adsorption species in subsurface soils may also be evidence of the

soil's erosional stability since reactive clay and soil surfaces require adequate residence time to adsorb Zn (Miranda-Treviono and Coles, 2003; Vespa et al., 2010).

In the high erodibility surface soils, Zn is present primarily as franklinite. The combination of aeolian and hydrological erosional effects combined with soil acidity greatly limits the formation of adsorption species for this class of soils. Water movement downslope erodes the labile Zn, increasing the relative abundance of franklinite. Soil acidity limits the formation of Zn precipitates, while adsorption is limited to complexes of very low points of zero charge (i.e. Si oxides) (Feng et al., 2007; Jacquat et al., 2008; Jacquat et al., 2009a; Alvarez et al., 2011).

Soils from the upper slope position (e.g., Site 5) appear to have lower total Zn concentrations due to downslope erosional losses. However, the speciation in the upslope surface soils is not significantly different from mid and lower slope surface soils. Instead, slope position has the much stronger influence on Zn speciation in the subsurface of erodible soils. At upper slope position (Site 5), surface soil is being removed not deposited; this Zn in the subsurface is the result of leaching through the soil as  $\text{Zn}^{2+}$ . This is also supported by the formation of Zn-Al-HIM in this Site 5 subsurface soil, as it would have required both aqueous Zn and  $\text{Al}^{3+}$  to precipitate (Jacquat et al., 2009a). In contrast, Zn speciation in subsurface lower slope soils is nearly identical to surface speciation.

In the mid slope high erodibility positions, surface and subsurface speciation is nearly identical due to the deposition of eroding soil from up-slope positions. The surface soil of these mid slope sites is eroded topsoil from up slope positions, while the subsurface soil is older buried surface or eroded soil. Although soils from Sites 3 and 6 have similar slope positions and speciation at the surface, there is more variability in Zn speciation of the subsurface soils. For the soil from Site 6, the presence of Zn adsorbed to soil Si and Mn oxides in the subsurface soil may indicate that the buried soil has more reactive surface sites for adsorption. Zinc speciation in the lower slope positions was identical to the mid-slope positions for both Site 3 and 6, which indicates that soil in the lower slope positions is mostly franklinite-rich eroded topsoil from the upslope soils.

#### **3.4.4 Zinc stability and environmental significance**

The persistence of the primary Zn minerals (franklinite and sphalerite) in all of the soils is a key observation. In the vegetation stabilized depressional soils, franklinite is still a significant component of the total Zn, but multiple secondary adsorption Zn species also were present. These adsorption complexes were observed to correspond to higher  $\text{CaCl}_2$  exchangeable Zn, and are expected to be labile in the field at low soil pH (Manceau et al., 2000; Jacquat et al., 2009a; Voegelin et al., 2011). Chemical weathering of franklinite will continue to release  $\text{Zn}^{2+}$ , but this process is slow in Flin Flon as evidenced by franklinite persistence after decades of exposure to the environment (Alloway, 1995). The remaining franklinite may provide a significant continued source of potentially labile/phytotoxic Zn as it weathers (Roberts et al., 2002).

The Zn adsorption species, both outer-sphere adsorbed Zn and inner-sphere complexes on Si and Mn oxides, appear to strongly correlate with the quantity of Zn desorbed from  $\text{CaCl}_2$  extractions (plant available). This fraction of Zn has the highest potential for being both mobile and phytotoxic (Bhattacharya et al., 2006; Churakov and Daehn, 2012), and the stabilized soils have a high relative abundance of the total Zn in this fraction. Stabilizing Zn in these soils will likely require either a significant pH increase (to above pH 6.5) to form Zn-Al layered double hydroxides or Zn carbonates or the addition of a highly reactive amendment at low pHs (Manceau et al., 2000; Nachtegaal et al., 2004; Degryse et al., 2011). The majority of Zn in these soils should be responsive to a significant shift in soil pH and/or an application of a highly reactive amendment capable of adsorbing Zn (Cheung et al., 2000; Fawzy, 2008; Jacquat et al., 2009b).

The high erodibility soils have similar Zn species as the stabilized soils; the differences lay in relative abundances of Zn species (the high erodibility soils are higher in franklinite) and in total Zn concentration (the high erodibility soils are much lower in total Zn than are the stabilized soils). These soils are also more acidic, which increases the risk of Al toxicity to plants (Miller and Watmough, 2009). The high relative abundance of franklinite and sphalerite indicate that much of the primary Zn minerals have not yet chemically weathered (Roberts et al., 2002). Although the total Zn concentration in these soils is significantly decreased, Zn release from weathering of the smelter-deposited minerals will still limit vegetative growth. The low relative abundance of outer-sphere Zn correlates with the low

amount of  $\text{CaCl}_2$  extractable Zn in these soils. This may indicate that Zn is not the main phytotoxic element; Al may also have a significant role in limiting revegetation for these sites.

At two of the sites, one stabilized and one highly erodible, a Zn-Al HIM co-precipitate was observed in the subsurface soils. This provides evidence that conditions in the landscape are conducive to form this extremely stable species (Scheinost et al., 2002). Zinc-Al-HIM formed in Flin Flon soils that had low total Zn concentration and soil pH near 4, although it has been shown to form in other soils at concentrations up to  $\sim 2000 \text{ mg Zn kg}^{-1}$  (Jacquat et al., 2009c). The natural formation of Zn-Al-HIM is significant because it is known to be a stable mineral under acidic conditions that typify both the natural boreal forest soils and smelter-acidified soils (Lothenback et al., 1997; Scheinost et al., 2002). Because Zn-Al-HIM reduces the phytotoxicity of both Zn and Al, formation of this species may encourage revegetation of some smelter affected areas, especially in the high erodibility soils.

### 3.5 Conclusions

Detailed molecular-scale Zn speciation of soils from the smelter-impacted landscape at Flin Flon MB provides insights into potential Zn phytotoxicity limiting the natural recovery of this boreal forest ecosystem. The application of synchrotron-based Zn speciation with landscape-scale observations provides ideas on the linkages between Zn transformations and pedological processes. Zinc speciation is dominated by the smelter-released minerals franklinite and to a lesser extent sphalerite. These minerals are slowly releasing  $\text{Zn}^{2+}$  into the soil environment via dissolution, but they persist even after decades of exposure due to the sub-arctic climate, acidic conditions, and soil pedogenic processes. Throughout the smelter-affected landscape, the dominant control on Zn speciation is soil pH. The soil acidity, especially in high erodibility landscape positions, has limited the transformation of Zn into secondary species and physical erosional transport processes have dominated Zn speciation and concentration. The high erodibility soils have a lower relative abundance of labile and total Zn due to the physical weathering from wind and water that has increased the relative abundance of franklinite and reduced the total concentration of Zn.

In the vegetation-stabilized soils where soil pH is slightly less acidic, transformation of Zn from franklinite into secondary adsorption species is far more prevalent. The stabilized

soils act as a collection point for the eroding/redistributed Zn from upper slope positions; this contributes to the high Zn concentrations and high labile Zn fractions. Because soil pedogenic processes are occurring in these stabilized soils, it is hypothesized that the weathering products of the Zn minerals (i.e., labile outer-sphere Zn and inner-sphere adsorption complexes) accumulates in these soils.

The formation of neo-phase Zn precipitates in two of the subsurface soils suggests that a larger natural attenuation process may be facilitated to occur at the Flin Flon site. The formation of a relatively insoluble Zn-Al-HIM would reduce the phytotoxic effects of labile Zn and Al. The acidic surface soil pH is likely the major limit on Zn-Al-HIM formation in eroding sites, while in stabilized soils high organic matter may limit Al availability. The stability of Zn-Al-HIM under acidic conditions makes it a desirable endpoint species for Zn in the Flin Flon landscape, and optimizing soil management practices to stimulate this phase's stability will be desirable.

## **4 EFFECTS OF DOLOMITIC LIMESTONE APPLICATION ON ZINC SPECIATION IN A BOREAL FOREST SMELTER CONTAMINATED LANDSCAPE**

### **4.1 Preface**

In the previous chapter characterization studies of soils from across the Flin Flon, MB smelter affected area revealed that Zn speciation correlates with landscape observations, mainly the potential for soil erosion. Speciation in high erodibility sites is dominated by the primary mineral franklinite as a result of soil erosion and leaching of the byproducts of franklinite weathering. Stabilized/depressional landscape areas were characterized as having a higher relative abundance of secondary Zn adsorption species that are far more labile under a  $\text{CaCl}_2$  extracting solution. To date, little is known about the interactions of Zn and the effects of liming on Zn speciation in boreal forest soils. This chapter addresses this by studying the effects of liming on Zn speciation through a field based chronosequence dating back ten years.

### **4.2 Introduction**

Zinc contamination from mining and smelting activities has led to severe ecological damage in many different types of ecosystems throughout the world. The Flin Flon, MB smelter affected area is one such contaminated landscape that cover approximately 10,000 ha (Henderson et al., 1998; McMartin et al., 1999). In addition to extensive heavy metal and acid deposition that are typical of the contamination associated with smelting, several large forest fires in the 1940s contributed to the initial forest dieback. However, the boreal forest ecosystem has been unable to recover naturally at this site due, at least in part, to high concentrations of heavy metals and soil acidity. In some of areas of the landscape, metal tolerant grasses have outcompeted the natural boreal forest vegetation, whereas other areas of the landscape remain bare of vegetation altogether. The challenges facing this metal contaminated site are predominantly high phytotoxic metal concentrations, primarily Zn, and acidic soils that occur as a result of sulfuric acid deposition (Henderson et al., 1998; McMartin et al., 1999; Scheinost et al., 2002).

It is known that speciation and not total concentration often governs the toxicity of heavy metals in the environment (Basta et al., 2005). This is because speciation strongly influences both the lability and bioavailability of Zn to organisms (Manceau et al., 2000; Roberts et al., 2002; Basta et al., 2005). Synchrotron-based X-ray Absorption Spectroscopy (XAS) is an analytical tool that has been successfully used by many researchers to elucidate Zn speciation in contaminated soils (Manceau et al., 2000; Roberts et al., 2002; Sarret et al., 2004; Vespa et al., 2010; Degryse et al., 2011; Voegelin et al., 2011). Both near edge (XANES) and extended (EXAFS) regions of an XAS spectrum can be used to examine Zn speciation; in both cases and for heterogeneous soils, linear combination fitting (LCF) can be used to semi-quantitatively determine the relative amounts of different mineral phases present by comparison of unknowns to a large library of reference compounds (Manceau et al., 2000; Jacquat et al., 2009a; Voegelin et al., 2011). For Zn samples with speciation that consist of primary smelter phases (e.g., franklinite and sphalerite), the XANES spectra may provide enough information for LCFs, but commonly soil Zn speciation is dominated by adsorption complexes or neophase precipitates that have similar XANES fingerprints. In these cases, LCF of the entire EXAFS region is preferable since EXAFS is more sensitive to the subtle differences in contribution from different atomic backscatters (Manceau et al., 2000, Voegelin et al., 2011). The LCF approaches alone may not always provide a unique solution and thus it can be difficult to choose and refine a model (Manceau et al., 2000) without additional chemical information. Other supporting information can be obtained by laboratory-based extraction methods (i.e. desorption studies, calcium chloride or sequential chemical extractions) that infer metal speciation indirectly based upon extractability (Scheinost et al., 2002; Voegelin et al., 2002; Sing et al., 2006). This provides standalone chemical information on the availability of Zn as well as validation of the LCF models (Manceau et al., 2000; Jacquat et al., 2009b; Sivry et al., 2010; Voegelin et al., 2011).

Zinc speciation in smelter contaminated soils has been extensively characterized via XAS spectroscopy, and several general observations from those studies can be made. Regardless of ecosystem, Zn speciation from smelter contamination is dependent on the initial ore composition. Zinc is primarily deposited in the landscape as franklinite, an iron rich spinel mineral ( $\text{ZnFe}_2\text{O}_4$ ) or as sphalerite, a  $\text{ZnS}$  mineral (Scheinost et al., 2002; Roberts et al., 2002; Jacquat et al., 2009a). The weathering of these smelter deposited minerals releases  $\text{Zn}^{2+}$



into the soil solution after which a variety of different secondary Zn species have the potential to form (Scheinost et al., 2002; Jacquat et al., 2009a; Van Damme et al., 2010). Depending on pH and sorbent availability, Zn can form secondary adsorption complexes with soil Si, Mn or Fe (oxy) hydroxides, organic material, or clay minerals (Tschapek et al., 1974; Manceau et al., 2000; Feng et al., 2007; Jacquat et al., 2009a). The formation of secondary Zn precipitates is also possible depending upon soil pH and the mineralogy of the soil. At acidic soil pH (4-4.5) and relatively moderate Zn contamination ( $\sim 2000 \text{ mg kg}^{-1}$ ) the formation of Zn-Al-hydroxy interlayer material (HIM) is common (Lothenbach et al., 1997; Scheinost et al., 2002; Jacquat et al., 2009c). In near neutral soils (pH 6.5) and higher Zn contamination levels, Zn-Al-layer double hydroxide (LDH) are more commonly found (Manceau et al., 2000; Voegelin et al., 2002; Jacquat et al., 2008; Voegelin et al., 2011).

The formation of secondary precipitates is an important attenuation process for reducing Zn phytotoxicity (Manceau et al., 2000; Roberts et al. 2002; Scheinost et al., 2002; Jacquat et al., 2009c; Voegelin et al., 2011). The formation of soil precipitates is dependent on the type of sorbent materials and is heavily influenced by reaction kinetics (Barrow, 1998; Scheckel et al., 2000; Scheckel and Sparks, 2001; Roberts et al., 2003; Nachtegaal and Sparks, 2004). The sorbent is responsible for the type of soil precipitate formed, for example the study by Scheckel and Sparks (2001) found the availability of Al in gibbsite allowed for the formation of LDH's while an  $\alpha$ -hydroxide formed on the non-Al containing mineral talc. The effect of temperature on the formation of soil precipitates increases the time required to form and stabilize the precipitate or adsorption species (Scheckel and Sparks, 2001). The effect of time in the reaction kinetics of soil precipitates has been shown to increase the relative abundance of the precipitate until equilibrium is reached but more importantly aging has shown to increase the stability of the precipitate (Scheckel et al., 2000; Nachtegaal and Sparks, 2004). The effect of temperature on reaction kinetics requires the approach of using a multi-year chronosequence in studying the effect of pH on Zn speciation in a sub-arctic climate.

Soils from the Flin Flon, MB smelter affected area have previously (Chapter 3) been classified into two distinct groups, (1) high erodibility and (2) stabilized (metal tolerant vegetation). These two soil groups have different vegetation growth responses to liming agents: high erodibility soils respond quickly to pH increases while stabilized soils have yet to respond to a lime application after an eleven year period. Because these are operational

definitions based on vegetative growth, it is important to understand the effect that liming has upon Zn speciation in these soils. A community led initiative, the Flin Flon, MB and Creighton, SK *Green Project*, has applied dolomitic limestone to aid revegetation of many areas of the smelter affected landscape over the last ten years. As a result of these activities, it is possible to sample chronosequences of high erodibility and stabilized soil catenas that have been limed. Because Zn fractionation in soils is heavily dependent upon soil pH, this study should reveal transitions between Zn species as the pH increases to neutral or slightly alkaline pH (Jacquat et al., 2009a). The objective of the study is to determine: (1) changes in Zn speciation in response to carbonate additions on two distinct soil types, and (2) the relationship/effectiveness of liming on soil catena chronosequences on potential Zn phytotoxicity and long-term stability.

## **4.3 Materials and Methods**

### **4.3.1 Site and soil selection**

The stabilized chronosequence site is located 1 km northeast of the processing facility. This is also the prevailing wind direction and the soil has high Zn concentrations ( $\sim 23,000 \text{ mg kg}^{-1}$ ). Dolostone has been applied at various times to sections of this site over an eleven year period, with sampling occurring in 2011. The main visual characteristic of the site is the presence of a metal tolerant grass species that stabilizes the soil from further erosion and also collects eroding soil. This chronosequence area has a uniform topography with only minor landscape features tending towards concave features.

The high erodibility chronosequence is located 3 km south of the processing facility in an area where Zn concentrations are typically less than  $2000 \text{ mg kg}^{-1}$  soil. Although soil Zn concentrations are lower than in the stabilized chronosequence, this site is unable to support plant growth without the application of a carbonate. The lack of vegetation results in soil erosion from upper slope (both concave and convex) positions into the depression/low laying positions. Much of the soil present at this site is located in shallow convex pockets on the hill slopes, with limited rhizosphere development and nutrient availability. Even with these constraints, however, high erodibility sites often rapidly establish vegetation after the Green project carbonate application. The large variability in topographical landscape positions and features for this chronosequence site presents an experimental challenge since both Zn

concentration and speciation are affected by slope position (Chapter 3). Soils were collected from the chronosequence sites with two 10 cm cores per collection point. The top 2 cm of both cores were composited for XAS and wet chemical measurements. Sample replicates are internal subsamples from the bulk.

#### **4.3.2 Carbonate and application methods**

The carbonate agent used at the field sites was a dolomitic limestone,  $\text{Ca,Mg}(\text{CO}_3)$ . The dolostone is a heterogeneous mixture of powder and gravel sized particles; its choice was due to local availability rather than effectiveness as a liming agent. Dolostone has been applied throughout the Flin Flon area since 2001 by the *Flin Flon MB/Creighton SK Green Project*. The *Green Project* is a local community group committed to the goal of revegetating the smelter impacted landscape. Community volunteers applied the dolostone by spreading buckets of material on the soil and thus the true application rate per site and per year is largely unknown. However, records of the location and timing of lime all applications were available, allowing our study to construct chronosequences. The stabilized chronosequenced catena is more complete with regular liming over a longer period of time than the high erodibility chronosequenced catena which has gaps in the 2-7 year range. However, the high erodibility catena has a sufficient number of sampling points and variation in the liming dates to determine how Zn speciation has been influenced over time. The major advantage of the selected study sites is they were both initially limed at nearly the same time (one year apart).

#### **4.3.3 Soil analysis**

Soil pH was measured using a 0.01 M  $\text{CaCl}_2$  background solution, with a ratio of 10:1(v/w) solution to soil (Nachtegaal et al., 2005; Jacquat et al., 2009a). The slurry was mixed over 0.5 h and then left to settle for 2 h before pH measurement (Nachtegaal et al., 2005; Jacquat et al., 2009a).

The operationally defined “plant available” fraction was completed using a batch replenishment extraction with 0.1 M  $\text{CaCl}_2$  adjusted to pH 4.5 with 0.1 M  $\text{HNO}_3$  (Strawn and Sparks, 2000; Nachtegaal et al., 2005). The batch extraction entailed of 1 g soil being extracted three separate steps with 35 mL replenishments shaken for 20 hrs at 100 RPM; after which the solution was filtered with 0.2  $\mu\text{m}$  disposable filters. The 100 mL  $\text{g}^{-1}$  replenishment

conditions were experimentally determined using a miscible displacement desorption experiment (Eick et al., 1999; Roberts et al., 2002).

The resultant supernatants were diluted (as needed) prior to analysis with a 4100 Microwave Plasma Atomic Emission Spectrometer [Agilent Technologies (Mississauga, ON)]. Total metal concentrations were determined using a Microwave digester and the traditional EPA method 3051; 9ml of 37% HCl and 3ml of 65% HNO<sub>3</sub> for a volume of 12 mL per 0.5 g of soil (Chen and Ma, 1998). The resultant supernatant solution was filtered to a pore size of 0.2 µm, and then diluted for analysis on a 4100 Microwave Plasma Atomic Emission Spectrometer [Agilent Technologies (Mississauga, ON)].

#### **4.3.4 XAS Data collection and analysis**

X-ray absorption spectroscopy data was collected at the Canadian Light Source (CLS) synchrotron in Saskatoon, SK. The CLS storage ring operates at 2.9 GeV and with a ring current of 250-150 mA. Bulk XAS measurements were collected at the HXMA beamline (06ID-1). Measurements were made at the Zn K-edge (9659 eV) with a Si-220 monochromator detuned by 50% to suppress higher order harmonics. The monochromator was calibrated to the first inflection point of the Zn K-edge Zn from a standard reference foil at 9659 eV. A spectrum of the standard reference foil was simultaneously collected with each XAS scan to correct for any variation in energy shifts between scans and samples.. Spectra collected from concentrated Zn standards were collected in transmission mode as a way of avoiding the self-absorption effects of fluorescence data. These concentrated standards were diluted to ensure an edge between 1.5 and 2 and were in powder form to minimize the potential for pin holes. Zinc standards and the soil samples themselves were measured using fluorescence mode and a 32-element Ge detector. To improve signal to noise quality with the Ge detector, a Cu-6 filter and Soller slits were placed between the sample and detector as a means of reducing scattering and unwanted fluorescence from other elements. Additionally, when collecting XAS spectra of Fe containing compounds/soils, Al foil was inserted between the sample and detector to further reduce undesired Fe fluorescence. A minimum of two scans were collected of each sample to ensure good data quality and to verify that beam damage effects were not occurring over the scans.

All XAS spectra for the study were analyzed with the ATHENA software package (Ravel and Newville, 2005). Data processing was completed with an initial inspection of individual detector channels, next, each scan was deglitched, and then a background was removed. Each spectra was then calibrated to the Zn reference foil (9659 eV), then aligned using the first derivative of the XANES spectra, and then merged. The EXAFS spectra were extracted using a  $k^3$ -weighted chi function over a range of 2-12  $k$  ( $\text{\AA}^{-1}$ ) after background subtraction and spline fitting. Data analysis was performed using the semi-quantitative approach of Linear Combination Fitting (LCF) routines on XANES and EXAFS data. The EXAFS fit range was dependent upon data quality but, typically was completed on a 2-12  $k$  ( $\text{\AA}^{-1}$ ) range. The fitting range for XANES data was between 9639-9759 eV. More details on the LCF approach and the library of Zn reference spectra used in the LCF analysis can be found in Appendix A.

## **4.4 Results and Discussion**

### **4.4.1 Effect of dolostone application on soil pH**

Soil pH and  $\text{CaCl}_2$  extractable metal concentrations are reported in Table 4.1. The dolostone application in the chronosequences increased soil pH in relation to the control soils that received no liming agent. In the high erodibility soil catena, the pH increase occurs quickly with an increase from 3.6 to 4.9 in less than a year. After this initial increase, additional time fails to further increase soil pH. After 7 years, which is the second sampling point of the chronosequence, soil pH has reverted to 3.6. These soils are potentially buffered back to pH 3.6 due to the presence of soluble aluminum sulfate salts in the soil. The formation of these aluminum salts in the pH 3.6-4.5 range would release  $\text{H}^+$  ions and lower the soil pH after dolostone application (Singh and Brydon, 1968; Xu et al., 2006; Adele et al., 2011). This is a potential explanation for the initial soil pH range for these soils being buffered in the 3.6 range, as there should be sufficient amounts of sulfate in the soils as a product of sulfuric acid deposition to form aluminum sulfate precipitates. This could represent a long-term buffering capacity of the soil back near pH 3.6. Alternatively, this could be explained as an erosional effect since this 0-2 cm soil is from a mid-slope position and the drop in pH could be due to the translocation of acidic soil from up-slope un-limed concave slope positions. In the 8-year, sample, the pH was 4.8, and the final sampling point after 10 years of liming had soil pH 5.7. The inconsistent soil pH response to liming for this site highlights the challenge of effectively liming landscapes where redistribution of acidic

Zn contaminated soil is occurring. However, it is important to also note that vegetation across this site responds quickly to liming and even a small pH increase (to pH 4.5) is sufficient to initiate boreal forest revegetation.

**Table 4.1. Soil pH and CaCl<sub>2</sub> extractable concentrations of the chronosequenced liming sites.**

Years since liming	Soil pH	CaCl <sub>2</sub> Extractable <sup>†</sup>	
		Zn	Al
	± 0.1	mg kg <sup>-1</sup> soil	
High Erodibility:			
Control (no dolostone) <sup>‡</sup>	3.6	55 ± 5	228 ± 24
1 <sup>§</sup>	4.9	55	0
7 <sup>§</sup>	3.6	50	218
8 <sup>§</sup>	4.8	55	5
10 <sup>‡</sup>	5.8	195 ± 23	9 ± 9
Stabilized/depressional:			
Control (no dolostone) <sup>§</sup>	4.3	15740	180
2 <sup>§</sup>	4.4	7950	80
3 <sup>‡</sup>	4.6	2320 ± 354	110 ± 28
9 <sup>‡</sup>	5.2	6142 ± 634	90 ± 8
10 <sup>§</sup>	5.7	1750	80
11 <sup>§</sup>	6.1	300	70

<sup>†</sup>pH 4.5 0.1 M CaCl<sub>2</sub> extractable metal (n=3)

Internal subsamples for CaCl<sub>2</sub> extractions: <sup>‡</sup>n=3, <sup>§</sup>n=1

In contrast, dolostone application in the vegetation stabilized chronosequenced catena caused a gradual but steady increase in soil pH. The initial pH of the stabilized control is almost 1 unit higher than the initial high erodibility control soil (4.3 vs. 3.6) which may indicate either a higher buffering capacity or decreased acid deposition on this site. The consistent soil pH increase (Table 4.1) from pH of 4.3 to 6.1 is consistent with soil erosion/deposition not significantly adding acidity to this chronosequence. While the incremental pH increase from year to year is small, the effect on  $\text{CaCl}_2$  extractable Zn is much larger. This demonstrates the important role of soil pH on Zn speciation on this chronosequence as well, although the mechanisms may potentially be different (Manceau et al., 2000; Jacquat et al., 2009a).

#### **4.4.2 Zinc XAS speciation**

Due to low Zn concentrations in the high erodibility soils, only near edge spectra were used for LCF analysis. The bulk XANES from the high erodibility chronosequence are shown in Fig. 4.1, and the best LCF models are tabulated in Table 4.2. A visual comparison of the bulk XANES for the chronosequence indicates that a change in Zn speciation has occurred. Two features of the XANES that substantiate a speciation shift: in the spectra of the “8 years since liming” soil a (1) decreased intensity of the triplet peaks at the edge 9660-9675 eV, associated with franklinite. (2) The development of an additional weak shoulder at 9710 eV that is denoted with a line on Fig. 4.1.

For stabilized soils, both XANES and EXAFS regions were utilized in the LCF modeling; LCF was performed on the EXAFS data (Fig. 4.2) and the best fit EXAFS models (tabulated in Table 4.2) were also compared to the XANES data (Fig. 4.3) to ensure the results were consistent with the near edge data as well. Visually, the EXAFS of the stabilized soils (Fig. 4.2) indicate that speciation changes accompanied increases in pH and aging. Two regions in the EXAFS at 5 and 7  $\text{k} (\text{\AA}^{-1})$ , seem particularly sensitive to changes in speciation when franklinite is present. The visual similarity between much of the EXAFS also is a consequence of the strong backscattering features of the franklinite ( $\text{ZnFe}_2\text{O}_4$ ), this species is known to partially mask the EXAFS contributions of other adsorption species (Manceau et al., 2000, Jacquat et al., 2009a). Nonetheless, the LCF EXAFS model simulates the XANES

spectra of the stabilized soils quite well without changing parameters (Fig. 4.3), which increases the confidence in the fit results.

To better visualize the changes in Zn speciation from XAS, LCF results were compared to changes in pH, time, and CaCl<sub>2</sub> extractable Zn in Fig. 4.4 (left). The stabilized soils increase in pH from pH 4.3 to 6.1 over an eleven-year period, and the pH increases are associated with three distinct Zn speciation regimes that are also consistent with changes in CaCl<sub>2</sub> extractable Zn (Jacquat et al., 2009b). The initial pH increase to 4.9 after 2 years corresponds with substantial adsorption of Zn on soil Mn oxides in the LCF model and resulted in a significantly lower concentration of CaCl<sub>2</sub> extractable Zn compared to the control. After 3 years the soil pH continued to increase and extractable Zn continued to decrease. As the pH increased above 5 in years 9-11, Zn adsorption on Fe oxide surfaces becomes more favourable due to the abundance of Fe oxides, but Zn adsorbed on Fe-oxides is more readily desorbed/exchanged than is Zn adsorbed on Mn oxides (Nachtegaal and Sparks, 2004; Feng et al., 2007). After eleven years the pH has risen to 6.1, and Zn speciation indicated a Zn-Al-LDH soil precipitate combined with the increase in all sorption species has reduced the amount of CaCl<sub>2</sub> extractable Zn to 300 mg Zn kg<sup>-1</sup> soil.

The high erodibility chronosequence results are also visualized in Fig.4.4 (right). The pH values of the high erodibility soils were less consistent than the stabilized site, probably due to re-acidification that accompanies erosional deposition. One year after liming, Zn-Al-HIM forms as a substantial component, and this species continues to increase in relative abundance over time. There is little change in the concentration of CaCl<sub>2</sub> extractable Zn from the control and the first 8 years of liming on the high erodibility site; the effect of HIM formation was instead noticeable in decreased CaCl<sub>2</sub> extractable Al (Table 4.1).



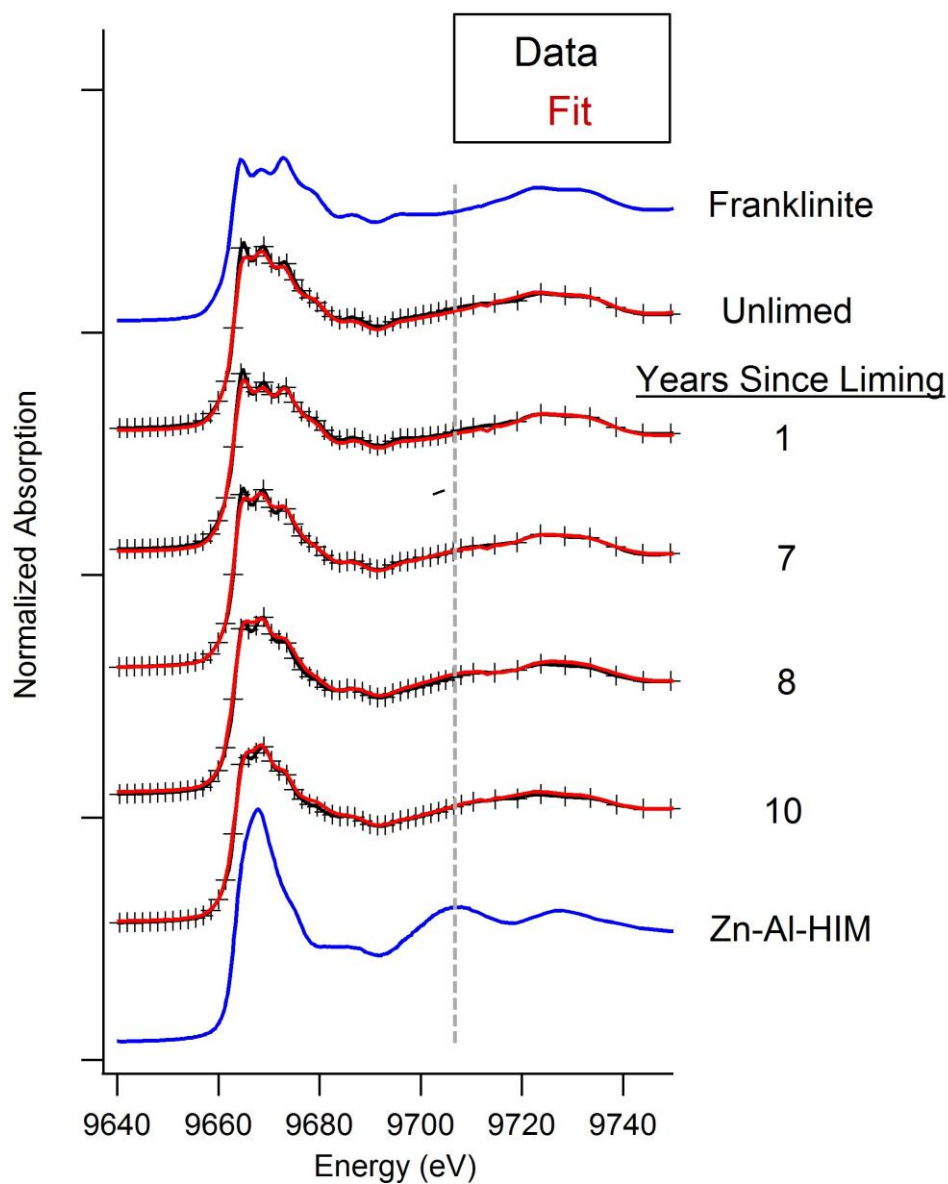


**Fig. 4.1. Bulk Zn XANES of the high erodibility chronosequence soils. Experimental data is shown by black crosses, and the LCF results are shown with a red line. The dashed line at 9710 eV highlights a shoulder feature that is diagnostic for neo-phase Zn-Al-HIM precipitate. For comparison, a Zn-Al-HIM and franklinite standard are shown in blue.**

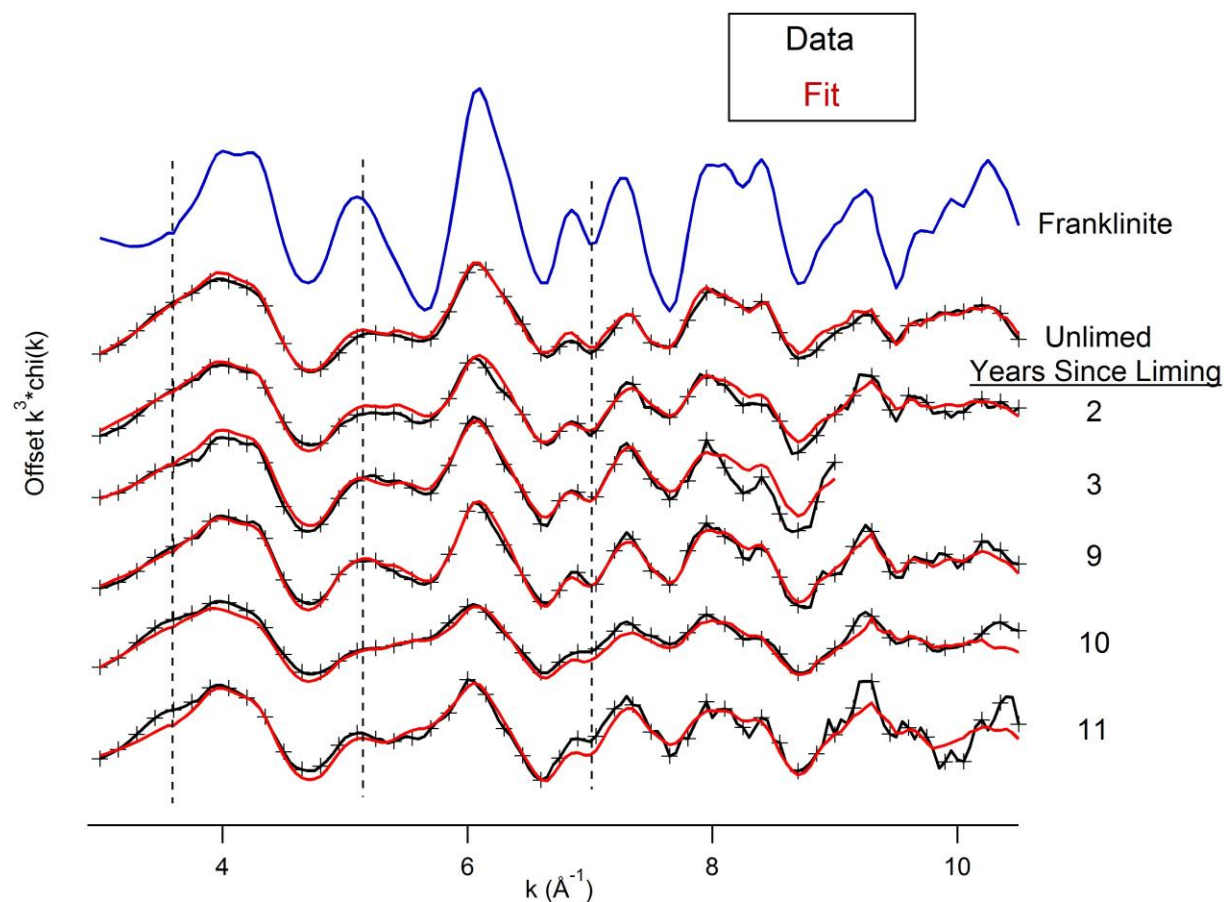


**Fig. 4.2.** Bulk Zn  $k^3$ -EXAFS (black) and LCF results (red) of the vegetation-stabilized chronosequence soil catena. The EXAFS of the “3 years since liming” spectra was limited to 9k ( $\text{\AA}^{-1}$ ) to ensure the LCF model wasn’t affected by signal quality. For reference,  $k^3$ -EXAFS of franklinite are shown in blue, and dashed lines denote regions diagnostic for franklinite in the EXAFS spectra of the chronosequence soils.

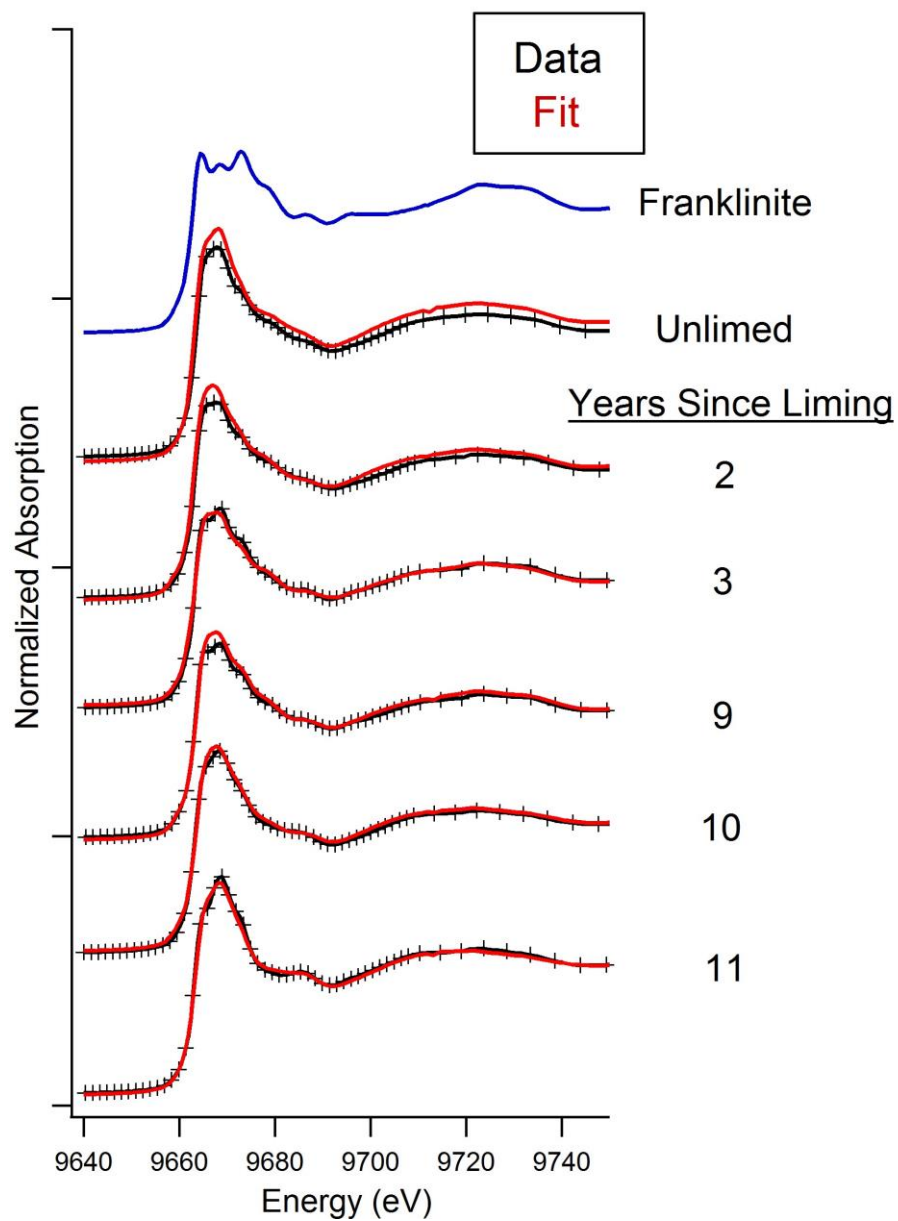


**Fig. 4.3. Bulk Zn XANES of the vegetation-stabilized chronosequence soil catena.**  
**Experimental data is shown by black crosses, and the LCF results are shown with a red line.**  
**For comparison, a franklinite standard is shown in blue.**

**Table 4.2. Bulk XAS LCF results of the chronosequence soil catenas.**

Years since liming	pH	CaCl <sub>2</sub> <sup>†</sup> extractable Zn	Franklinite (ZnFe <sub>2</sub> O <sub>4</sub> )	Sphalerite	Zn- LDH	Zn- CO <sub>3</sub>	Zn- HIM	Zn-Sorbed				Reduced Chi <sup>2</sup>
								SiO <sub>2</sub>	FeOOH	MnO <sub>2</sub>	Outer- sphere/ Zn <sup>2+</sup> <sub>(aq)</sub>	
High Erodibility:	± 0.1	mg kg <sup>-1</sup>					% <sup>‡</sup>					XANES <sup>¶</sup> or EXAFS <sup>#</sup>
Control	3.6	55 ± 5	79	-	-	-	-	-	-	-	25	7×10 <sup>-4¶</sup>
1	4.9	55	76	14	-	-	13	-	-	-	-	2×10 <sup>-4¶</sup>
7	3.6	50	63	-	-	-	25	13	-	-	-	3×10 <sup>-4¶</sup>
8	4.8	55	49	15	-	-	35	-	-	-	-	2×10 <sup>-4¶</sup>
10	5.8	195 ± 23	48	10	-	20	-	-	-	-	23	2×10 <sup>-4¶</sup>
Stabilized:												
Control	4.3	15740	37	-	-	-	-	23	-	-	50	0.39 <sup>#</sup>
2	4.4	7950	28	-	-	-	-	10	-	43	22	0.33 <sup>#</sup>
3 <sup>§</sup>	4.6	2320 ± 354	36	15	-	-	-	-	-	23	26	0.53 <sup>#</sup>
9	5.2	6142 ± 634	37	-	-	-	-	-	15	36	12	0.25 <sup>#</sup>
10	5.7	1750	16	-	22	-	-	-	29	33	-	0.21 <sup>#</sup>
11	6.1	300	23	-	42	-	-	-	-	37	-	0.92 <sup>#</sup>

<sup>†</sup>Extractable Zn with a pH 4.5±0.1 0.1M CaCl<sub>2</sub> extracting solution.

<sup>‡</sup>% Relative contribution to XAFS signal, models unconstrained.

<sup>§</sup>Linear combination fit to 9k (Å<sup>-1</sup>).

<sup>¶</sup>Linear combination fit model of XANES data -20 to +100eV from the absorption edge (9569 eV).

<sup>#</sup>Linear combination fit model of EXAFS data 2-12k (Å<sup>-1</sup>).

In the final year of liming, soil pH increased to 5.7, and a Zn carbonate precipitate formed instead of Zn-Al-HIM. It is known that Zn carbonate is less stable than Zn-Al-HIM under acidic conditions; this is likely the reason that the Year 11 soil has the highest concentration of extractable Zn (Jacquat et al., 2009b). Because the dolomite persists in Flin Flon as discrete particles, the Zn carbonate fraction may be the result of the formation of a hydrozincite mineral on the dolomite surface (Jacquat et al., 2009b).

#### **4.4.3 Effect of liming on Chronosequence Zn speciation**

The general effects of liming on Zn speciation in both the high erodibility and stabilized soil catenas illustrate the importance of pH and time on contaminant fate (Manceau et al., 2000; Jacquat et al., 2009a). The wide diversity of observed Zn species is due to a combination of increased sorbent reactivity and increased precipitate stability as pH is increased. The liming agent produced mixed results in terms of the effect on soil pH in the high erodibility and stabilized soil catenas. In the high erodibility catena, 11 years of dolomitic weathering has altered Zn speciation sufficiently to facilitate regrowth of typical boreal forest plant species, but this change in vegetation occurred without drastically altering the concentration of  $\text{CaCl}_2$  extractable Zn. In contrast, liming of the stabilized soil catena drastically changed the soil Zn speciation and  $\text{CaCl}_2$  extractable Zn without significantly altering the vegetation on this site.

Based upon XAS results, the explanation for why high erodibility soils have good plant response to a liming agent is primarily the formation of Zn-Al-HIM precipitates. The relative abundance of HIM increases with time, suggesting that Zn-Al-HIM is able to continue precipitating long-term with additional Zn and Al inputs from erosional deposition. The formation of Zn-Al-HIM appears to have a maximum relative abundance of 35%, while the  $\text{CaCl}_2$  extractable Zn and Al data suggests that the limitation may be due to Al availability, not Zn. This is consistent with findings of Scheinost and coworkers (2002). From Table 4.1, Zn is still extractable eleven years after liming while extractable Al has fallen below 10 mg Al  $\text{kg}^{-1}$ . The ideal 3:1 Al:Zn ratio of Zn-Al-HIM requires a large pool of available  $\text{Al}^{3+}$  for the formation of HIM (Scheinost et al., 2002; Jacquat et al., 2009c).

The gradual pH increase across the stabilized chronosequence is evidence of the liming agent slowly overcoming the soil's acidic buffering capacity. This slow dissolution of dolostone reaches a nearly optimal pH for reducing Zn phytotoxicity in soils (Jacquat et al., 2009a; Vespa et al., 2011; Voegelin et al., 2011) after 11 years. Because Zn speciation in this site was initially ~50% outer-sphere surface complexes, these soils have a large pool of reactive Zn that can respond to pH increases (Nachtegaal et al., 2005; Jacquat et al., 2009c). The major effect of the gradual pH increases on this chronosequence, however, is to change the type of sorbent minerals present. This shift in Zn adsorbents observed with XAS correlates well with the abundance and known points of zero charge (PZC) of various soil minerals. Prior to liming, the acidity of the control unlimed soil limits adsorption sites to Si oxides and outer-sphere complexes on permanently-charged clay mineral exchange sites. As liming increases the pH increases above the PZC of Mn oxides, much of the outer-sphere Zn begins to instead adsorb to these reactive sites (Feng et al., 2007). As pH increases above 5, available Zn begins to sorb on the increasingly reactive and abundant soil Fe oxides. Zinc-Fe oxide adsorption complexes are stable above pH 5, but pH 4.5 CaCl<sub>2</sub> extraction will lead to desorption and to the release of Fe oxide bound Zn into the soil solution. When the pH increases to above 5.6, Zn-Al-LDH precipitates formed; the relative abundance of LDH phases increased further at pH 6. The stability of the Zn-Al-LDH phase has been well documented in literature (Manceau et al., 2000; Roberts et al., 2002; Roberts et al., 2003; Voegelin et al., 2005; Jacquat et al., 2008) and the formation of Zn-Al-LDH in our samples was accompanied by a large decrease the concentrations of Zn desorbed via CaCl<sub>2</sub> extraction. Calcium chloride extractions from the stabilized chronosequence demonstrate that increasing soil pH above 6 can significantly lower Zn solubility for the stabilized soils.

#### **4.4.4 Long term effects of liming on Zn phytotoxicity**

Since the overall goal of liming in Flin Flon is to facilitate natural boreal forest vegetative growth, it is important to form stable mineral/sorption species that are resistant to future acidification. Zinc stabilization, indirectly measured by CaCl<sub>2</sub> extraction, is accomplished with the formation of stable Zn mineral species Zn-Al-HIM and Zn-Al-LDH. These species once formed appear to be resistant to a CaCl<sub>2</sub> pH 4.5 extraction. However, the mechanisms responsible for precipitating either Zn-Al-HIM or Zn-Al-LDH are significantly different with respect to total Zn levels, final soil pH and soil mineralogy (Jacquat et al., 2009c). Despite

the potential limitations, one of these two precipitate species is capable of forming in many of the contaminated areas of Flin Flon, and thus represents a stable end-point that can reduce Zn phytotoxicity in both vegetatively stabilized and high erodibility soils.

Liming of the high erodibility chronosequence soils led to revegetation and eventual soil stabilization on this chronosequence, which also reduce erodibility and thus the future spread of contaminated soil on these sites. The management of high erodibility soils only requires a slight pH increase to 4-4.5, which reduces the deleterious effects of both Zn and Al through Zn-Al-HIM co-precipitation (Jacquat et al., 2009c). The stability of Zn-Al-HIM under acidic conditions (pH 3.5-4.5) ensures Zn and Al will remain stable with natural mineral weathering or upon the release of organic acids from boreal forest vegetation (Augusto et al., 1998; Jacquat et al., 2009c).

The major long-term effect of liming on the stabilized soil chronosequence is to reduce  $\text{CaCl}_2$  extractable Zn to levels where boreal forest regrowth is possible. Since metal tolerant grass exists in these stabilized soils and initial pH is above 4, very little Al is available for formation of Zn-Al-HIM phases and exchangeable Zn remains high (6,000-15,000  $\text{mg kg}^{-1}$ ) until the soil pH is increased to 5.7-6 after 10 years and Zn-Al-LDH forms. Once Zn-Al-LDH forms in the soil, exchangeable Zn levels are lowered dramatically (Roberts et al., 2003). To stimulate this reaction, the stabilized soils would benefit from either a more effective liming agent or a more regular application of dolomitic lime to rapidly raise soil pH to 6 or higher.

#### **4.5 Conclusions**

The chronosequence sites provide evidence for variable effect of pH and time on Zn speciation in Flin Flon soils. The highly erodible Flin Flon soils typically have lower Zn concentration; moreover, vegetation (within a year) responds to the application of a liming agent. The mechanism for this positive plant response appears to be dissolution of the franklinite mineral species and the rapid precipitation of Zn-Al-HIM, which occurs with only a minor pH increase. Formation of Zn-Al-HIM influences both Zn and Al solubility and this allows boreal forest revegetation on these soils to flourish even if the soil is subsequently re-acidified. The continued long-term dissolution of the liming agent on high erodibility sites has little long term benefit other than the continuation of Zn-Al-HIM precipitation until either the exchange sites of the smectite clay or Al availability is exhausted (Scheinost et al., 2002).

Al toxicity appears to be as limiting as Zn in the success of vegetation establishment throughout this chronosequence. In contrast, the stabilized chronosequence soils require nearly a decade of contact with the liming agent before boreal forest vegetation can compete with the existing metal-tolerant grasses. In these soils, reducing Zn phytotoxicity may require more intensive management practices such as additional and/or higher quality liming inputs or addition of sorbent amendments. For example, addition of smectite clays could stimulate Zn-Al-HIM formation and addition of sorbents such as zeolites or bonechar could provide substantially more sorption capacity for Zn at low pH.



## 5 SYNTHESIS AND GENERAL DISCUSSION

### 5.1 General Zn speciation in Flin Flon

Revegetation of the Flin Flon, MB smelter affected landscape has been limited by Zn phytotoxicity. Because toxicity is dependent upon speciation (Basta et al., 2005) using XAS to characterize Zn speciation and determine the mechanisms of Zn bonding in the soil environment can aid in the development of revegetation management techniques. The dominant Zn species in Flin Flon, MB soils are: (a) franklinite formed and released during the smelting process and (b) Zn adsorbed on soil minerals resulting from franklinite and sphalerite dissolution. These soils have also been acidified by sulfuric acid deposition; and thus acidic conditions have combined with the sub-arctic climate to limit both the weathering of the primary Zn minerals and the progression of natural attenuation processes. As a result, Zn speciation in these soils is not comparable to similar Zn smelter affected landscapes from temperate climates with circumneutral soil pH (Manceau et al., 2000; Roberts et al., 2002; Jacquat et al., 2009a; Jacquat et al., 2009b). The sub-arctic climate conditions are expected to slow the reaction kinetics required for natural attenuation of Zn that is a prerequisite for the reforestation of this landscape.

Initial Zn speciation in the Flin Flon soils was largely franklinite, which was present throughout the landscape in high relative abundances (50-85%). Franklinite must be relatively stable in the Flin Flon soil environment given its widespread persistence, but the slow weathering of this mineral has also been a continuous source of labile Zn (Alloway 1995; Jacquat et al., 2009a). Soil acidity has limited the reactive sites available to adsorb and/or precipitate available labile Zn (Manceau et al., 2000; Jacquat et al., 2008; Jacquat et al., 2009a). Although the released Zn is more available and thus more phytotoxic than franklinite, it is also a required component for natural attenuation to occur via formation of less soluble secondary precipitates. Without the chemical weathering of franklinite and

subsequent formation of stable secondary Zn species, Zn will continue to be a limitation on the revegetation of the Flin Flon landscape.

The second mineral species found in many Flin Flon soils was sphalerite, ZnS. Sphalerite typically occurs as a 10-15% component of LCF models when present and was more often observed in depressional soils from lower landscape positions. The accumulation of sphalerite was likely the result of soil erosion that concentrates this mineral in landscape positions where it was less susceptible to chemical weathering (Chapter 3; Voegelin et al., 2011; Liu et al., 2012). Although the initial quantities of franklinite and sphalerite in the smelter emissions are unknown, the much lower relative abundance of sphalerite in soils may be evidence that it is more susceptible to weathering (Roberts et al., 2002; Acero et al., 2007; Voegelin et al., 2011). In any case, the low concentrations and relative abundances of sphalerite present in the studied soils should have little future effect on the revegetation of these soils as it appears to have already weathered into secondary labile Zn species.

The presence and stability of adsorption complexes in soils is strongly dependent on soil pH (Roberts et al., 2003; Manceau et al., 2004; Jacquat et al., 2009a). The dominant adsorption complex found throughout the Flin Flon soils was Zn adsorbed as an outer-sphere complex on clay mineral surfaces. This adsorption complex forms electrostatically on the CEC sites of soil minerals and is thus pH and mineralogy dependent (Jacquat et al. 2009a). This Zn species would be  $\text{CaCl}_2$  exchangeable and thus labile in the soil profile (Scheinost et al., 2002).

The two adsorption complexes that were found to form in the soils of Flin Flon are Zn adsorbed on Si and Mn oxides. The low PZC of Si oxides allow for the formation of this adsorbed species throughout soils of the contaminated area (Tschapek et al., 1974; Miranda-Trevino and Coles, 2003). This adsorption species is only present as a minor component, which indicates that the adsorptive capacity of Si oxides may be low in these soils. Furthermore, this complex is believed to be exchangeable with high ionic strength  $\text{CaCl}_2$  extracting solutions, based on mass calculations of desorbed vs. total Zn. The second adsorption species is Zn adsorbed on Mn oxide minerals. This Mn oxide sorbent has a slightly higher PZC than  $\text{SiO}_2$  but when soil pH is high enough for them to react they are known to have a high capacity for Zn adsorption (Feng et al., 2007; Kwon et al., 2013).

Given a soil pH of around 4.5, this sorption complex was shown in the chronosequence liming study (Chapter 4) to adsorb a significant amount of Zn. Furthermore, this fraction was resistant to pH 4.5  $\text{CaCl}_2$  extraction and can be expected to reduce Zn lability.

## **5.2 High Erodibility Soils**

### **5.2.1 Landscape effect on Zn speciation**

Several factors are significantly affecting the concentration and chemical speciation of Zn in high erodibility soils. Interestingly, the speciation differences typically occur in the relative abundances of a few dominant Zn species rather than in the presence of many different components. The observed variation in Zn speciation relates to the effects of soil erosion (Chapter 3). Water movement through these soils selectively removes labile Zn into lower sloped positions, increasing the relative abundance of the mineral fractions of Zn (Chapter 3). As such, most of the labile outer-sphere fraction of Zn from upper concave positions will erode into lower convex positions. Soil deposition over time into the low-lying slope positions has likely buried previously contaminated soil, resulting in higher Zn concentrations at depth and similar speciation results to surface soils (Chapter 3). In the majority of cases throughout the landscape, the effects of erosion were closely linked to a positive plant growth response after liming.

Regardless of landscape position, highly erodible soils typically respond with a positive vegetation response after even minor and short term increases in soil pH. The effect of soil erosion has lowered the surface concentration of Zn, and increased Zn concentration at depth. The acidic pH of these soils (typically 3.5 to 3.9) is below the PZC of the most reactive soil adsorbents, greatly limiting the potential of adsorption complex formation (Jacquat et al., 2009a). As the chronosequence study demonstrated (Chapter 4), the effects of erosion may persist after liming, since treated areas can be re-contaminated/re-acidified via erosion from an untreated upslope area.

### **5.2.2 Reducing Zn phytotoxicity in high erodibility soils**

The management technique for reducing Zn phytotoxicity and promoting plant growth in highly erodible soils is increasing soil pH through the application of liming agents. The addition of a liming agent to these soils influences the speciation of Zn, reducing the potential for Zn phytotoxicity. As seen through Chapter 4, Zn and Al can rapidly form a Zn-Al-HIM

co-precipitate species with even minor pH increases. The precipitate readily forms in almost every studied eroding soil after the application of a liming agent (Chapter 4). Once formed, Zn-Al-HIM reduces the amount of  $\text{CaCl}_2$  extractable Zn and Al in our samples, and precipitation of Zn-Al-HIM as an effective mechanism for reducing Zn toxicity has been demonstrated in the literature for soils with less than  $2000 \text{ mg Zn kg}^{-1}$  soil and high  $\text{Al}^{3+}$  concentrations (Scheinost et al., 2002; Jacquat et al., 2009c). Ultimately, Zn-Al HIM formation requires the presence of all three components ( $\text{Zn}^{2+}$ ,  $\text{Al}^{3+}$ , and smectite clay), which may lower its widespread utility for Zn stabilization in Flin Flon.

In general, application of a liming agent to highly erodible soils, with sufficient time, results in successful revegetation. However, the formation of Zn-Al-HIM in these soils may not sequester all of the available Zn. Additional soil amendments may help further facilitate Zn-Al-HIM formation, beyond what readily forms in these soils with a pH increase to 4-4.5. Addition of the additional reactants required for Zn-Al-HIM formation (smectites clays or  $\text{Al}^{3+}$ ) may promote the further precipitation of Zn and/or available Al. It was noted during the chronosequence study (Chapter 4) that Al is essential in HIM formation; thus addition of amendments that outcompete Zn-Al HIM for Al may not reduce labile Zn. As an example, addition of organics that have a high affinity to complex with  $\text{Al}^{3+}$  could reduce Zn-Al-HIM formation (Alvarez et al., 2011; Collignon et al., 2012). To effectively manage the high erodibility Flin Flon soils, either a zeolite or smectite clay based amendment could be added in addition to the liming agent. These amendments are expected to further facilitate the formation of HIM in soils where it naturally forms, and could possibly stimulate formation in other soils.

## **5.3 Stabilized/depressional Soils**

### **5.3.1 Landscape effects on Zn speciation**

The second soil classification originates from areas that have been stabilized by metal tolerant grasses. These soils typically have higher Zn concentration from their depressional location, which serves as a collection point from upslope positions, and they typically also have a higher relative abundance of secondary Zn species (Chapter 3). Zinc movement within these soils is limited to leaching of labile Zn downwards in the soil profile. The majority of Zn contamination remains in the top few centimetres of the soil profile, whereas at a depth of

8-10cm, Zn was found as secondary adsorption species in much lower concentrations (Chapter 3). The challenge in revegetation for these stabilized soils is in significantly reducing the Zn concentrations to facilitate boreal vegetation growth. High exchangeable Zn concentrations persist even after liming, as seen in the initial liming of stabilized soils from the chronosequence study (Chapter 4). Even after eleven years of dolostone dissolution, the soil pH increased to above 6 but liming was generally ineffective in promoting plant growth. These soils failed to precipitate Zn-Al-HIM in any sample (Chapters 3 and 4) likely due to an increase in organic matter from the metal tolerant grasses that reduces the  $\text{Al}^{3+}$  availability (Jacquat et al., 2009c; Jacquat et al., 2009a; Alvarez et al., 2011). The effect of soil pH on Zn speciation in stabilized soils is fairly consistent with the speciation of contaminated sites of temperate climates (Manceau et al., 2000; Jacquat et al., 2009a).

### **5.3.2 Reducing Zn phytotoxicity in stabilized soils**

The initial pH increase after liming favours Zn adsorption on Mn oxides and decreases the amount of  $\text{CaCl}_2$  extractable Zn. However, Mn oxide adsorption sites/concentration, are insufficient to adsorb the quantity of available Zn in these soils, and phytotoxicity effects persist. Further pH increases result in Zn adsorbing on Fe oxide surfaces. Iron oxides have significantly more adsorptive capacity, concentration effect, than Mn oxides allowing for higher relative abundances (Nachtegaal and Sparks, 2004). Although, it was found that the resulting Zn-Fe oxide adsorption species desorb in a pH 4.5  $\text{CaCl}_2$  extracting solution indicating that this Zn is still potentially plant available (Chapter 4). After eleven years of exposure to the dissolving liming agent, the pH increase resulted in formation of a Zn-Al-LDH precipitate that stabilized a high percentage of the total Zn. Initially in the unlimed stabilized soil,  $\sim 15,000 \text{ mg Zn kg}^{-1}$  soil was extracted with  $\text{CaCl}_2$  from the untreated soil, but in the chronosequence soil with LDH formation, extracted Zn dropped to  $\sim 300 \text{ mg Zn kg}^{-1}$  soil (Chapter 4). This demonstrates that Zn speciation in stabilized soils will eventually respond to pH increases, but these soils require a significantly higher pH than the highly erodible soils.

During the chronosequence study, the time needed to produce a pH above 6 in the stabilized soils largely explains the slow changes in speciation and  $\text{CaCl}_2$  extractable Zn. The slow/non-existent boreal vegetation recovery on these soils indicates that more intensive

management may be beneficial. For example, the process of forming Zn-Al-LDH phases under the chronosequence conditions requires a decade, and the formation of this phase has not yet translated into positive growth response of boreal forest species. To speed Zn-Al-LDH precipitation, a more effective liming agent (or more frequent lime applications) may be necessary. In addition to liming, a reactive amendment (i.e., a phosphorous amendment) may also reduce the amount of  $\text{CaCl}_2$  extractable Zn by directly adsorbing labile from the soil solution. One such amendment may be the addition of a meat and bone meal biochar, which has shown promise in Flin Flon soils as a remediation amendment. Phosphorus based biochars have been shown to be effective in sorbing high concentrations of Zn and may prove effective in reducing labile Zn from soils where Zn-Al-HIM cannot form (Cheung et al., 2000).

## 6 CONCLUSION

Zinc speciation in the Flin Flon, MB smelter-impacted area is affected by soil pH, pedogenic soil erosion processes and climate. Soil acidity has limited the reactive sites of minerals in the soil and the formation of stable/non-labile secondary Zn species. High rates of soil erosion on the deforested slope positions combined with the introduction of invasive metal tolerant grasses in largely depressional/level landscape positions has produced two distinct regions of influence on Zn speciation. The highly erodible soils are characterized by a high potential for both wind and water erosion; whereas metal tolerant grass stabilized sites act as a collection point for the eroding upslope soils. The Zn in both landscape classifications even after decades of environmental exposure, is largely present as a mixture of (a) smelter deposited (primary) Zn minerals franklinite and sphalerite and (b) secondary Zn phases that form from chemically weathered Zn released from the mineral phases. The differences originate from the relative amounts of these two Zn forms and the stability of the secondary phases that are present. For high erodibility soils, much of the labile Zn is leached into downslope convex positions that effectively concentrate the relative abundance of mineral phases and reduces the total Zn concentration in the residual soil. In contrast, stabilized soils have a significantly higher Zn concentration and increased relative abundance of labile and secondary adsorption Zn species.

The high erodibility soils develop as a result of boreal forest being unable to recolonize these mid/up slope positions due to the highly acidic soil pH and Zn and Al phytotoxicity. This allows for erosion to continue and preferentially leach Zn and soil downslope. This movement of soil results in the periodic burial of low slope position surface soils and accumulation of both Zn and eroded soil. The process for reducing phytotoxicity in these soils is the addition of liming agent that raises the soil pH between 4-4.5 where Zn-Al-HIM rapidly forms Zn-Al-HIM. The rapid formation, stability at acidic pH, and resistance to

natural weathering in the environment make Zn-Al-HIM well suited as an endpoint for Zn in these soils.

Zinc speciation in stabilized non-eroding soils is similar to that of the highly erodible soils; the major difference is in the relative abundances of the mineral and secondary Zn species. The stabilized sites have higher concentrations of Zn from the collection of soil from nearby eroding areas. These conditions have selectively allowed metal tolerant grass species to invade and flourish. This classification of soils requires a significant shift in pH-dependent Zn speciation for revegetation with native species. The chronosequence study demonstrated that dolostone liming agents have a gradual pH increasing effect and may be able to effectively influence Zn speciation towards non-exchangeable species after a decade of reaction.

For both highly erodible and stabilized soils, the effect of pH on Zn speciation in the Flin Flon landscape is pronounced and is the dominant factor that can shift Zn from labile to non-labile forms. In some cases, only a minor pH shift is required to facilitate the formation of non-exchangeable Zn-Al-HIM species; in others a significant increase beyond the typical range for boreal forest soils must be achieved before reduced Zn availability can occur. The related effects of time and climate on Zn speciation and revegetation are also important. The persistence of franklinite, and the slow effect of dolostone to increase the soil pH to ~6 suggest that reaction kinetics are significantly slower in Flin Flon than in temperate ecosystems. The sub-arctic climatic conditions appear to have simultaneously slowed the weathering of franklinite, and the secondary natural attenuation processes resulting in large areas of the landscape that still have high concentrations of phytotoxic Zn. This demonstrates that a significant amount of time will be required for natural forest revegetation to be successful in the Flin Flon landscape regardless of the revegetation strategy that is adopted.

Future research regarding Zn speciation in the Flin Flon landscape is required to fill in some missing links in site characterization and to ensure that the soils will react to pH increases as predicted. Additional Zn speciation data could also be used to create speciation maps of the ecosystem indicating the potential areas and the type of response that they would have to a liming agent or other amendment. Future work should also include developing an amendment that optimizes Zn-Al-HIM formation throughout the landscape including not only



the high erodibility sites but also the stabilized soils. The pH range of most Flin Flon soils are ideal for Zn-Al-HIM formation and using amendments that take advantage of this mineral phase to stabilize Zn would be a simpler solution than continual addition of liming agents. This could potentially be achieved with smectite clay, a zeolite, or an Al-rich smectite amendment to provide the framework materials for Zn-Al-HIM formation.

## 7 REFERENCES

- Abbaspour, A. and A. Golchin. 2011. Immobilization of heavy metals in a contaminated soil in Iran using di-ammonium phosphate, vermicompost and zeolite. *Environ. Earth Sci.* 63:935-943.
- Acero, P., J. Cama and C. Ayora. 2007. Sphalerite dissolution kinetics in acidic environment. *Appl. Geochem.* 22:1872-1883.
- Adele, M. J., R. N. Collins, T. D. Waite. 2011. Mineral species control of aluminum solubility in sulfate-rich acidic waters. *Geochim. Cosmochim. Acta.* 75: 965-977.
- Ajat, M.M.M., K. Yusoff and M.Z. Hussein. 2008. Synthesis of glutamate-zinc-aluminium-layered double hydroxide nanobiocomposites and cell viability study. *Curr. Nanosci.* 4:391-396.
- Alloway J. B. 1995. Soil processes and the behaviour of heavy metals. In: J.B. Alloway, editor, *Heavy metals in soil*, Second Edition. Blackie Academic and Professional. Bishopbriggs, Glasgow. p. 11-35.
- Alvarez, E., M. Fernandez-Sanjurjo, X. Luis Otero and F. Macias. 2011. Aluminum speciation in the bulk and rhizospheric soil solution of the species colonizing an abandoned copper mine in galicia (NW Spain). *J. Soils Sediments* 11:221-230.
- Augusto, L., P. Bonnaud and J. Ranger. 1998. Impact of tree species on forest soil acidification. *For. Ecol. Manage.* 105:67-78.
- Baker, L.R., G.M. Pierzynski, G.M. Hettiarachchi, K.G. Scheckel and M. Newville. 2012. Zinc speciation in proximity to phosphate application points in a Lead/Zinc smelter-contaminated soil. *J. Environ. Qual.* 41:1865-1873.
- Basta, N., J. Ryan and R. Chaney. 2005. Trace element chemistry in residual-treated soil: Key concepts and metal bioavailability. *J. Environ. Qual.* 34:49-63.
- Barrow, N. 1998. Effects of time and temperature on the sorption of cadmium, zinc, cobalt, and nickel by a soil. *Aust. J. Soil Res.* 36:941-950.
- Bhattacharya, A.K., S.N. Mandal and S.K. Das. 2006. Adsorption of Zn(II) from aqueous solution by using different adsorbents. *Chem. Eng. J.* 123:43-51.
- Chen, M. and LQ. Ma. 1998. Comparison of four USEPA digestion methods for trace metal analysis using certified and Florida soils. *J. Environ. Qual.* 27:1294-1300.
- Cheung, C., J. Porter and G. McKay. 2000. Sorption kinetics for the removal of copper and zinc from effluents using bone char. *Sep. Purif. Technol.* 19:55-64.
- Churakov, S.V. and R. Daehn. 2012. Zinc adsorption on clays inferred from atomistic simulations and EXAFS spectroscopy. *Environ. Sci. Technol.* 46:5713-5719.

- Ciszewski, D., U. Kubsik and U. Aleksander-Kwaterczak. 2012. Long-term dispersal of heavy metals in a catchment affected by historic lead and zinc mining. *J. Soils Sediments* 12:1445-1462.
- Collignon, C., J.-. Boudot and M.-. Turpault. 2012. Time change of aluminium toxicity in the acid bulk soil and the rhizosphere in norway spruce (*picea abies* (L.) karst.) and beech (*fagus sylvatica* L.) stands. *Plant Soil* 357:259-274.
- Degryse, F., A. Voegelin, O. Jacquat, R. Kretzschmar and E. Smolders. 2011. Characterization of zinc in contaminated soils: Complementary insights from isotopic exchange, batch extractions and XAFS spectroscopy. *Eur. J. Soil Sci.* 62:318-330.
- Eick, M., J. Peak, P. Brady and J. Pesek. 1999. Kinetics of lead adsorption/desorption on goethite: Residence time effect. *Soil Sci.* 164:28-39.
- Eisenberger, P. and B. Kincaid. 1978. EXAFS - new horizons in structure determinations. *Science* 200:1441-1447.
- Fawzy, E.M. 2008. Soil remediation using in situ immobilisation techniques. *Chem. Ecol.* 24:147-156.
- Feng, X.H., L.M. Zhai, W.F. Tan, F. Liu and J.Z. He. 2007. Adsorption and redox reactions of heavy metals on synthesized Mn oxide minerals. *Environ. Pollut.* 147:366-373.
- Ferreira Fontes, M.P. and G.C. dos Santos. 2010. Lability and sorption of heavy metals as related to chemical, physical, and mineralogical characteristics of highly weathered soils. *J. Soils Sediments* 10:774-786.
- Hardie, A.G., J.J. Dynes, L.M. Kozak and P.M. Huang. 2009. Biomolecule-induced carbonate genesis in abiotic formation of humic substances in nature. *Can. J. Soil Sci.* 89:445-453.
- Henderson, P., I. McMartin, G. Hall, J. Percival and D. Walker. 1998. The chemical and physical characteristics of heavy metals in humus and till in the vicinity of the base metal smelter at Flin Flon, Manitoba, Canada. *Environ. Geol.* 34:39-58.
- Impellitteri A. C., A. E. Herbert, Y. Yujun, Y. Sun-Jae, J. K. Saxe. 2001. Soil properties controlling metal partitioning. In: H.M. Selim and D. Sparks, editors. *Heavy metal release in soils*. Lewis Publishers. Boca Raton, FL. p. 149-166.
- Jacquat, O., A. Voegelin and R. Kretzschmar. 2009a. Soil properties controlling Zn speciation and fractionation in contaminated soils. *Geochim. Cosmochim. Acta* 73:5256-5272.
- Jacquat, O., A. Voegelin, F. Juillot and R. Kretzschmar. 2009b. Changes in Zn speciation during soil formation from Zn-rich limestones. *Geochim. Cosmochim. Acta* 73:5554-5571.
- Jacquat, O., A. Voegelin and R. Kretzschmar. 2009c. Local coordination of Zn in hydroxy-interlayered minerals and implications for Zn retention in soils. *Geochim. Cosmochim. Acta* 73:348-363.

- Jacquat, O., A. Voegelin, A. Villard, M.A. Marcus and R. Kretzschmar. 2008. Formation of Zn-rich phyllosilicate, Zn-layered double hydroxide and hydrozincite in contaminated calcareous soils. *Geochim. Cosmochim. Acta* 72:5037-5054.
- Khan, M.J. and D.L. Jones. 2009. Effect of composts, lime and diammonium phosphate on the phytoavailability of heavy metals in a copper mine tailing soil. *Pedosphere* 19:631-641.
- Kingery, L. W., A. J. Simpson, M. Hayes. 2001. Chemical Structures of Soil Organic Matter and Their Interactions with Heavy Metals. In: H. Selium and D. Sparks, editors. Heavy metal release in soils. Lewis Publishers: p. 237-244.
- Kwon, K.D., K. Refson and G. Sposito. 2013. Understanding the trends in transition metal sorption by vacancy sites in birnessite. *Geochim. Cosmochim. Acta* 101:222-232.
- Li, W., K.J.T. Livi, W. Xu, M.G. Siebecker, Y. Wang, B.L. Phillips and D.L. Sparks. 2012. Formation of crystalline Zn-Al layered double hydroxide precipitates on gamma-alumina: The role of mineral dissolution. *Environ. Sci. Technol.* 46:11670-11677.
- Limpijumnong, S., M.F. Smith and S.B. Zhang. 2006. Characterization of As-doped, p-type ZnO by X-ray absorption near-edge structure spectroscopy: Theory. *Appl. Phys. Lett.* 89:222113.
- Liu, J., S. Wen, Y. Xian, J. Deng and Y. Huang. 2012. Dissolubility and surface properties of a natural sphalerite in aqueous solution. *Miner Metall Process* 29:113-120.
- Manceau, A., M. Marcus, N. Tamura, O. Proux, N. Geoffroy and B. Lanson. 2004. Natural speciation of Zn at the micrometer scale in a clayey soil using X-ray fluorescence, absorption, and diffraction. *Geochim. Cosmochim. Acta* 68:2467-2483.
- Manceau, A., B. Lanson, M. Schlegel, J. Harge, M. Musso, L. Eybert-Berard, J. Hazemann, D. Chateigner and G. Lambelle. 2000. Quantitative Zn speciation in smelter-contaminated soils by EXAFS spectroscopy. *Am. J. Sci.* 300:289-343.
- McMartin, I., P. Henderson and E. Nielsen. 1999. Impact of a base metal smelter on the geochemistry of soils of the Flin Flon region, Manitoba and Saskatchewan. *Can. J. Earth Sci.* 36:141-160.
- Merila, P., M. Malmivaara-Lamsa, P. Spetz, S. Stark, K. Vierikko, J. Derome and H. Fritze. 2010. Soil organic matter quality as a link between microbial community structure and vegetation composition along a successional gradient in a boreal forest. *Appl. Soil Ecol.* 46:259-267.
- Miller, D.E. and S.A. Watmough. 2009. Soil acidification and foliar nutrient status of Ontario's deciduous forest in 1986 and 2005. *Environ. Pollut.* 157:664-672.
- Miranda-Trevino, J. and C. Coles. 2003. Kaolinite properties, structure and influence of metal retention on pH. *Appl. Clay. Sci.* 23:133-139.
- Nachtegaal, M. and D. Sparks. 2004. Effect of iron oxide coatings on zinc sorption mechanisms at the clay-mineral/water interface RID A-9709-2010. *J. Colloid Interface Sci.* 276:13-23.

- Nachtegaal, M., M. Marcus, J. Sonke, J. Vangronsveld, K. Livi, D. Van der Lelie and D. Sparks. 2005. Effects of in situ remediation on the speciation and bioavailability of zinc in a smelter contaminated soil. *Geochim. Cosmochim. Acta* 69:4649-4664.
- Nriagu, J., H. Wong, G. Lawson and P. Daniel. 1998. Saturation of ecosystems with toxic metals in Sudbury basin, Ontario, Canada. *Sci. Total Environ.* 223:99-117.
- Owojori, O.J., and S. Siciliano. 2012. Accumulation and toxicity of metals (copper, zinc, cadmium, and lead) and organic compounds (geraniol and benzo[A]pyrene) in the oribatid mite *oppia nitens*. *Environ. Toxicol. Chem.* 31:1639-1648.
- Petrovic, M., M. Kastelan-Macan and A. Horvat. 1999. Interactive sorption of metal ions and humic acids onto mineral particles. *Water Air and Soil Poll* 111:41-56.
- Pokrovsky, O.S., J. Viers and R. Freydier. 2005. Zinc stable isotope fractionation during its adsorption on oxides and hydroxides. *J. Colloid Interface Sci.* 291:192-200.
- Ramos Arroyo, Y.R. and C. Siebe. 2007. Weathering of sulphide minerals and trace element speciation in tailings of various ages in the Guanajuato mining district, Mexico. *Catena* 71:497-506.
- Ravel, B. and M. Newville. 2005. ATHENA, ARTEMIS, HEPHAESTUS: data analysis for X-ray absorption spectroscopy using IFEFFIT. *J. Synchrotron Radiat.* 12:537-541.
- Rehr, J. and R. Albers. 2000. Theoretical approaches to X-ray absorption fine structure. *Rev. Mod. Phys.* 72:621-654.
- Rigina, O., A. Baklanov, O. Hagner and H. Olsson. 1999. Monitoring of forest damage in the Kola Peninsula, northern Russia due to smelting industry. *Sci. Total Environ.* 229:147-163.
- Roberts, D., R. Ford and D. Sparks. 2003. Kinetics and mechanisms of Zn complexation on metal oxides using EXAFS spectroscopy. *J. Colloid Interface Sci.* 263:364-376.
- Roberts, D., A. Scheinost and D. Sparks. 2002. Zinc speciation in a smelter-contaminated soil profile using bulk and microspectroscopic techniques. *Environ. Sci. Technol.* 36:1742-1750.
- Sarret, G., J. Balesdent, L. Bouziri, J. Garnier, M. Marcus, N. Geoffroy, F. Panfili and A. Manceau. 2004. Zn speciation in the organic horizon of a contaminated soil by micro-x-ray fluorescence, micro- and powder-EXAFS spectroscopy, and isotopic dilution. *Environ. Sci. Technol.* 38:2792-2801.
- Scheckel, K. and D. Sparks. 2001. Temperature effects on nickel sorption kinetics at the mineral-water interface. *Soil Sci. Soc. Am. J.* 65:719-728.
- Scheckel, K., A. Scheinost, R. Ford and D. Sparks. 2000. Stability of layered Ni hydroxide surface precipitates - A dissolution kinetics study. *Geochim. Cosmochim. Acta* 64:2727-2735.
- Scheinost, A.C., R. Kretzschmar, S. Pfister and D.R. Roberts. 2002. Combining selective sequential extractions, X-ray absorption spectroscopy, and principal component analysis for quantitative zinc speciation in soil. *Environ. Sci. Technol.* 36:5021-5028.

- Singh, S. S. and J. E. Brydon. 1968. Solubility of basic aluminum sulfates at equilibrium in solution and in the presence of Montmorillonite. *Soil Science* Vol. 107, No. 1. 12-16.
- Sipos, P., T. Nemeth, V.K. Kis and I. Mohai. 2008. Sorption of copper, zinc and lead on soil mineral phases. *Chemosphere* 73:461-469.
- Sivry, Y., M. Munoz, V. Sappin-Didier, J. Riotte, L. Denaix, P. de Parseval, C. Destrigneville and B. Dupre. 2010. Multimetallic contamination from Zn-ore smelter: Solid speciation and potential mobility in riverine floodbank soils of the upper lot river (SW France). *Eur. J. Mineral* 22:679-691.
- Strawn, D. and D. Sparks. 2000. Effects of soil organic matter on the kinetics and mechanisms of Pb(II) sorption and desorption in soil. *Soil Sci. Soc. Am. J.* 64:144-156.
- Tschapek, M., L. Tcheichvili and C. Wasowski. 1974. Point of zero charge (pzc) of kaolinite and  $\text{SiO}_2 + \text{Al}_2\text{O}_3$  mixtures. *Clay Miner.* 10:219-229.
- Van Damme, A., F. Degryse, E. Smolders, G. Sarret, J. Dewit, R. Swennen and A. Manceau. 2010. Zinc speciation in mining and smelter contaminated overbank sediments by EXAFS spectroscopy. *Geochim. Cosmochim. Acta* 74:3707-3720.
- Vespa, M., M. Lanson and A. Manceau. 2010. Natural attenuation of zinc pollution in smelter-affected soil. *Environ. Sci. Technol.* 44:7814-7820.
- Voegelin, A., S. Pfister, A. Scheinost, M. Marcus and R. Kretzschmar. 2005. Changes in zinc speciation in field soil after contamination with zinc oxide. *Environ. Sci. Technol.* 39:6616-6623.
- Voegelin, A., A. Scheinost, K. Buhlmann, K. Barmettler and R. Kretzschmar. 2002. Slow formation and dissolution of Zn precipitates in soil - A combined column-transport and XAFS study. *Environ. Sci. Technol.* 36:3749-3754.
- Voegelin, A., O. Jacquat, S. Pfister, K. Barmettler, A.C. Scheinost and R. Kretzschmar. 2011. Time-dependent changes of zinc speciation in four soils contaminated with zincite or sphalerite. *Environ. Sci. Technol.* 45:255-261.
- Waychunas, G., C. Fuller and J. Davis. 2002. Surface complexation and precipitate geometry for aqueous Zn(II) sorption on ferrihydrite I: X-ray absorption extended fine structure spectroscopy analysis. *Geochim. Cosmochim. Acta* 66:1119-1137.
- Weng, C. and C. Huang. 2004. Adsorption characteristics of Zn(II) from dilute aqueous solution by fly ash. *Colloid Surface A* 247:137-143.
- XU, R. K., S.C. Xiao, J. Y. Li, D. Tiwari, and G. L. Ji. 2007. Hydrolysis of aluminum ions in kaolinite and oxisol suspensions as influence by organic anions. *Pedosphere* 17: 90-96.
- Yano, J. and V.K. Yachandra. 2009. X-ray absorption spectroscopy. *Photosynthesis Res.* 102:241-254.
- Zhang, G.Y. and D. Peak. 2007. Studies of Cd(II)-sulfate interactions at the goethite-water interface by ATR-FTIR spectroscopy. *Geochim. Cosmochim. Acta* 71:2158-2169.
- Zhang, S., H. Fortier and J. Dahn. 2004. Characterization of zinc carbonate hydroxides synthesized by precipitation from zinc acetate and potassium carbonate solutions. *Mater. Res. Bull.* 39:1939-1948.

## **APPENDIX A**

### **ZINC XAFS STANDARDS, LOADINGS, AND LINEAR COMBINATION FITTING METHODOLOGY**

### A.1. Precipitate standards

A Zn co-precipitated hydroxyl Interlayer Material (Zn-Al-HIM) was synthesized as per Scheinost et al. (2002). After synthesis, the resulting Zn-Al-HIM coprecipitate was washed to remove any unreacted  $\text{Zn}^{2+}$ .

The Zn-Al-LDH precipitate standard was prepared under a  $\text{N}_2$  atmosphere with a 3:1 Zn:Al ratio using  $\text{Zn}(\text{NO}_3)_2$  and  $\text{Al}(\text{NO}_3)_3$  (Mokrish et al., 2008). The precipitate was formed at pH 7 while adding the reactant solutions under mixing conditions; the resulting solution was heated for 18 hours at 70 °C (Mokrish et al., 2008). The precipitate was then vacuum filtered and triple washed with D.I. water.

$\alpha$ -Zn(OH)<sub>2</sub> was synthesized as per Waychunas et al.(2001); under a  $\text{N}_2$  atmosphere the pH of a 0.55 M  $\text{Zn}(\text{NO}_3)_2$  (pH 3.0) solution was slowly increased to 6.5 with  $\text{CO}_2$  free 1.0 M NaOH while stirring. The solution was then aged for 24-hrs at room temperature under  $\text{N}_2$  atmospheric conditions, the resultant precipitate was then vacuum filtered and triple rinsed with D.I. water to remove entrained ( $\text{Zn}^{2+}$ ) and dissolved nitrate.

The synthesis of  $\text{ZnCO}_3$  was performed as per Zhang et al. (2004), Briefly, a 1:1 of 0.05 M  $\text{Zn}(\text{NO}_3)_2$  and 0.05 M  $\text{K}_2\text{CO}_3$  solutions are mixed under vigorous stirring conditions at room temperature. The resulting precipitate was stirred for 1hr and then left still for 24 hrs, the  $\text{ZnCO}_3$  precipitate was vacuum filtered and triple washed with D.I. water removing any unreacted  $\text{Zn}^{2+}$ . The precipitate was dried, ground, and placed in a sealed container for storage until XAS measurements were collected.

Zn oxide and Zn phosphate were purchased as reagent grade dry precipitates from Fisher Scientific Canada.

### A.2. Sorption standards

Adsorption standards were prepared with mineral suspensions of 0.5g/L that were sparged with  $\text{N}_2$  in a 0.1 M  $\text{NaNO}_3$  background electrolyte. Initial pH was lowered to pH 5 to ensure that carbonate was removed from the system. Zinc was added (as  $\text{Zn}(\text{NO}_3)_2$ ) for a final concentration of 1 mM; after Zn addition the pH was slowly titrated to pH 6.5 under  $\text{N}_2$ . The bottles were sealed, shaken for 48hr, filtered and the solid residue was washed with 0.1 M



NaNO<sub>3</sub> to displace entrained Zn. A list of the loadings of the adsorption standards and surface areas of the sorbent phases can be found below (Table A.1).

The MnO<sub>2</sub> sorbent is a birnessite mineral previously synthesized and characterized (Hardie et al., 2009) and provided by Dr. J. Dynes. The goethite sorbent was provided by Dr. Peak and has been previously characterized (Zhang , G.Y. and D. Peak, 2007). The bonemeal biochar adsorption standard was characterized and provided by Aaron Betts.

**Table A.1. Loadings of Zn adsorption reference standards**

Mineral	Surface Area	Loading	Concentration
	m <sup>2</sup> g <sup>-1</sup>	μmol g <sup>-1</sup>	mg Zn kg <sup>-1</sup>
MnO <sub>2</sub>	63	47	3100
Fe(O)OH	63	39	2600
Na-Montmorillonite	-	16	1100
SiO <sub>2</sub>	860	42	2800
Bonemeal biochar	35	396	25894

### A.3. Mineral standards

Zinc minerals (franklinite, sphalerite, and willimite) were supplied from the University Of Saskatchewan Department Of Geology. All materials had identical EXAFS and XANES features noted in previously reported mineral standards from other sources (Manceau et al., 2000; Sheinost et al., 2002; Jacquat et al., 2009a). Zinc standards spectra can be found below in Fig. A.1. (XANES) and A.2. (EXAFS).

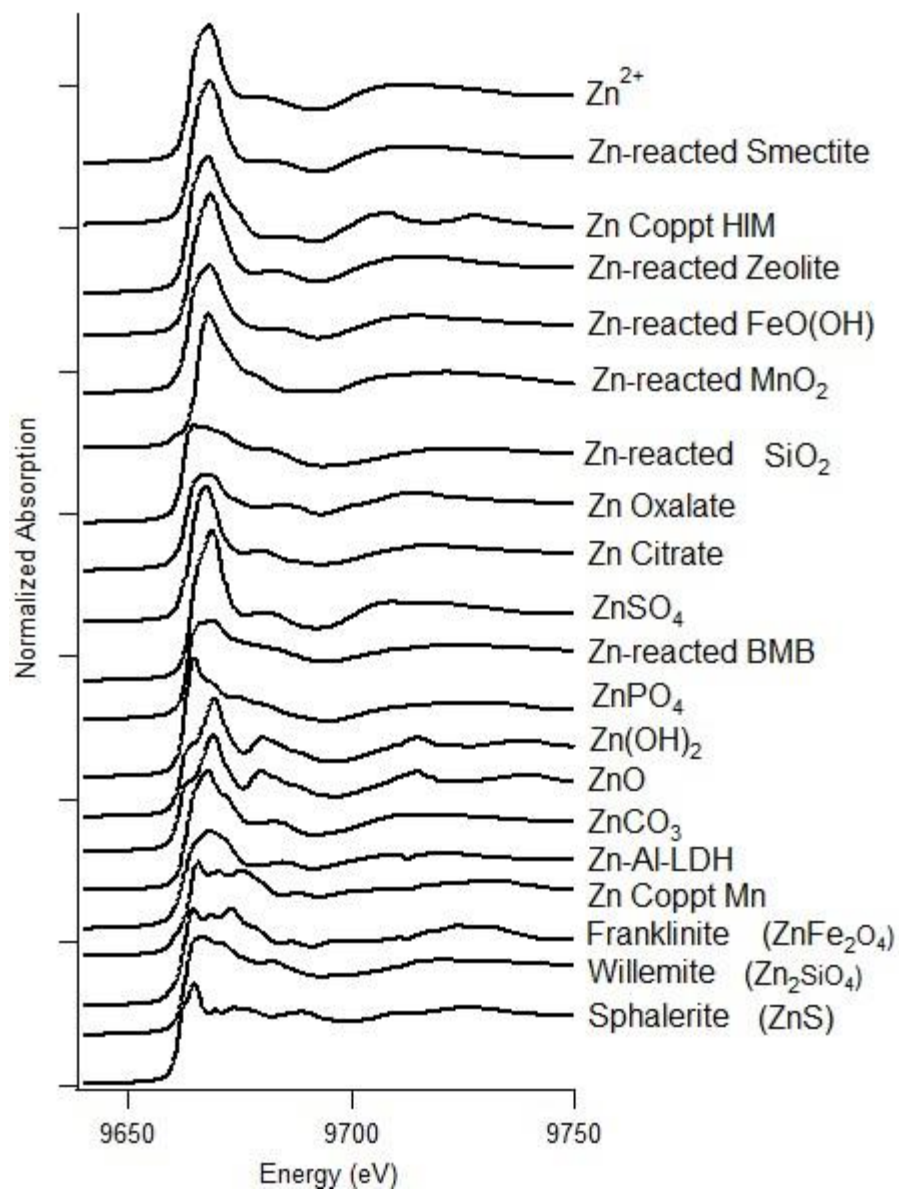


**Fig. A.1. Zinc reference standards, XANES spectra used in Linear Combination Fitting (LCF) of Flin Flon soil samples.**

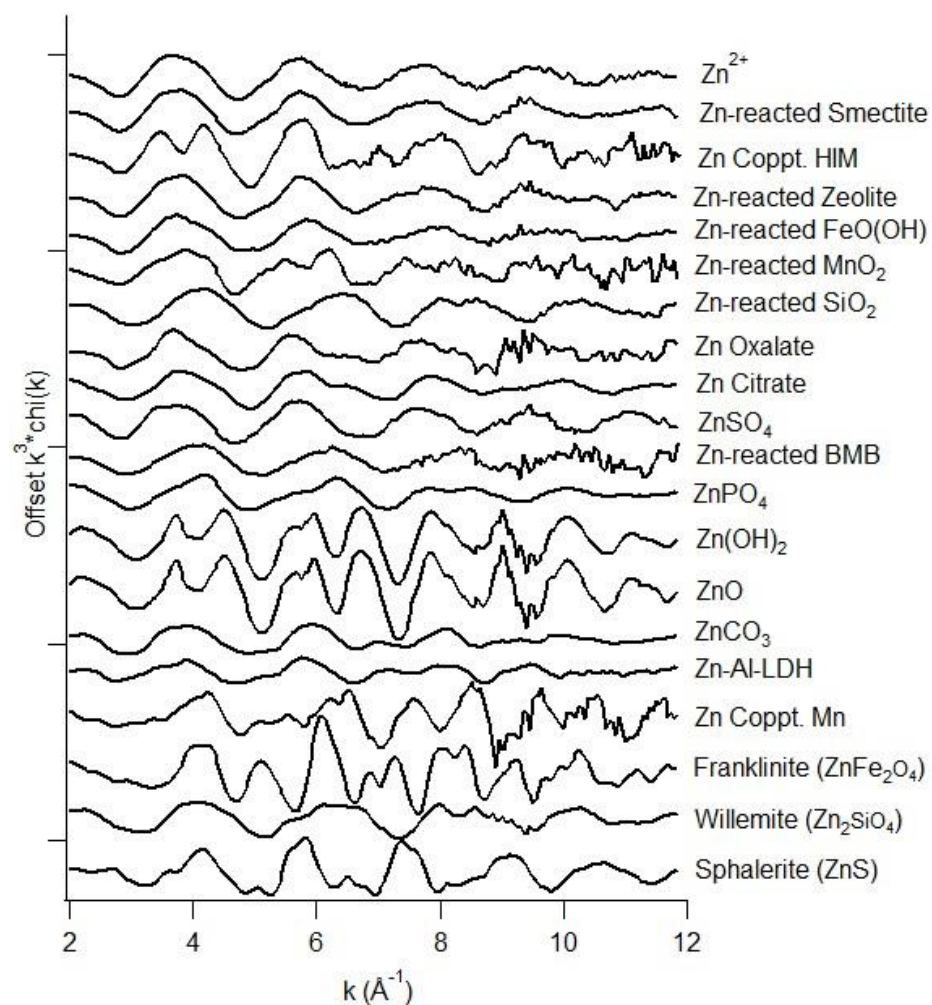


**Fig. A.2.** Zinc reference standards bulk EXAFS used in Linear Combination Fitting (LCF) of Flin Flon soil samples.

#### **A.4. Linear combination fitting rationale**

The challenges of selecting a final linear combination fit model are numerous due to the fitting program only using mathematical and statistical methods for selecting the best model fit. Because the ATHENA software is unable to incorporate additional chemical information into its fitting parameters, additional information must be subjectively utilized to determine the best possible model fit for each spectra. To increase the confidence in choosing a LCF model the following information is useful: total concentrations,  $\text{CaCl}_2$  (plant available) extractable concentrations, pH values, use of micro-XANES data identifying individual components (as a form of principle component analysis), point of zero charge (PZC) reactivity of potential adsorption complexes, and the potential conditions favoring specific species i.e., one particular precipitate over another. Using this information incorporates known chemical data into selecting the model fit, taking model fitting past purely relying on the statistical output of the fitting program.

The linear combination fitting approach used throughout this thesis for all XAS spectra is as follows: the parameters of the initial LC fits ( $E_0$  shift, large number of standards, model sum to 100%, and weight of each standard between 0% and 100%) were first unconstrained and allowed to vary; this was done to cut down on number/types of Zn species that obviously are not part of the spectra. The results were collected and compared against the model fits when increasing parameter constraints (i.e.,  $E_0$  shift equal for all standards in each fit) are applied. If when more constraints are applied the overall model fit drastically changes it implies the wrong reference standard where being used in the initial fit routine. Once a fairly stable model was developed, the standards used as part of that fit were then checked against expected species that form under the environmental conditions of that sample (i.e., soil pH, extractable concentrations, and total concentrations). As an example using soil pH, if the model fit contained a Zn-Fe adsorption complex when the soil pH was 3.5 this fit is chemically unlikely even if it had the best statistical fit. Using this subjective reasoning, unreasonable Zn species were eliminated and the model fits were further refined. The next step was to ensure that the EXAFS model fits (if EXAFS data was collected) were also good fits of the XANES spectra. If not further model refinement using different combination of

relevant standards to ensure that the final model fits explained reasonably well both XANES and EXAFS data, even if the chosen model was not the model programs best statistical fit.

Linear combination fitting typically has an uncertainty factor in the range of 10%. As a model test the data files of three Zn standards were added together at various percentages to one data file and then linear combination fit to determine the accuracy of the process. The modeling process was able to describe known mixtures to within 8% of the actual mixture. This lends confidence to model fits with components in the 10-15% range that these are actual real components of the data spectra.

## **APPENDIX B**

### **SUPPLEMENTAL TO CHAPTER 3: ZINC SPECIATION IN THE FLIN FLON LANDSCAPE**



**Fig. B.1.** Core used to collect surface and depth soil throughout the Flin Flon MB landscape, 10 cm in total length.





**Fig. B.2. Site 1 landscape photo. The area is characterized by metal tolerant grass species limiting the potential for soil erosion. Much of the metal tolerant grass had been removed for the development of amendment plots.**





**Fig. B.3. Site 2 landscape photo the site is characterized by metal tolerant grass species limiting soil loss from erosion and accumulation soil from the surrounding landscape positions.**



**Fig. B.4. Site 3 landscape photo, area is characterized by high potential rates of soil erosion. This site is located approx.. 1 km North and slightly east of the smelting and processing facility.**

## **APPENDIX C**

### **SUPPLEMENTAL TO CHAPTER 4:**

#### **EFFECTS OF APPLIED DOLOMITIC LIMESTONE WEATHERING ON ZN SPECIATION WITH TIME IN A SMELTER CONTAMINATED LANDSCAPE**

Additional XRF image maps used in determining Zn relationships in Flin Flon soils discussed in Chapter 4. Due to image size, page constraints and redundancies of displaying multiple similar XRF maps as part of Chapter 4 they are instead presented as supplemental information.

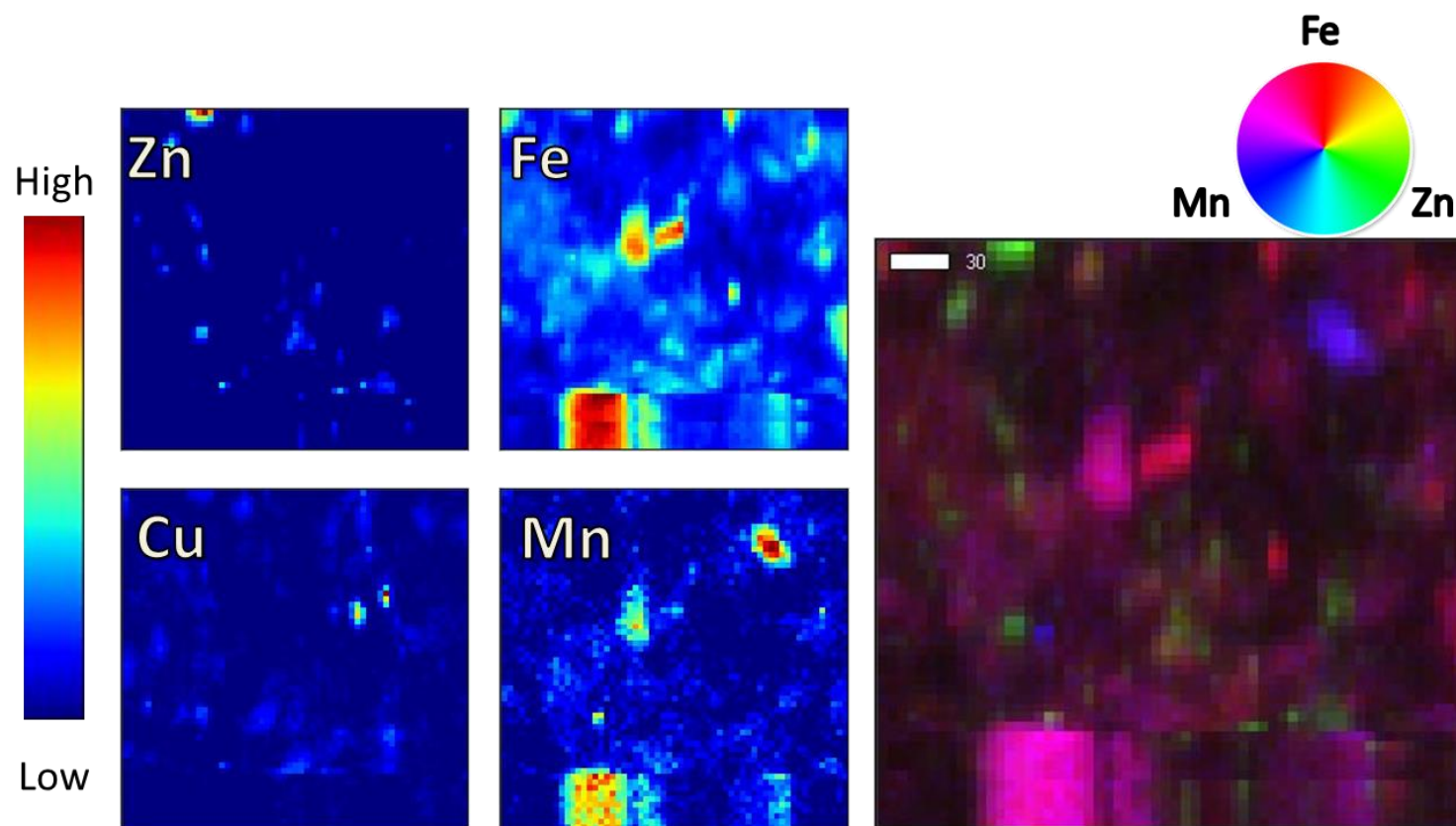


**Fig. C.1. Un-limed high erodibility surface soil (0-2 cm) synchrotron XRF microprobe maps for Zn, Fe, Cu, and Mn. Colors denote intensity (red = high relative elemental concentration, dark blue = low relative elemental concentration) and tri-colour maps (300 × 300 μm) reveal 2D spatial relationships of Zn, Fe, and Mn throughout the soil.**



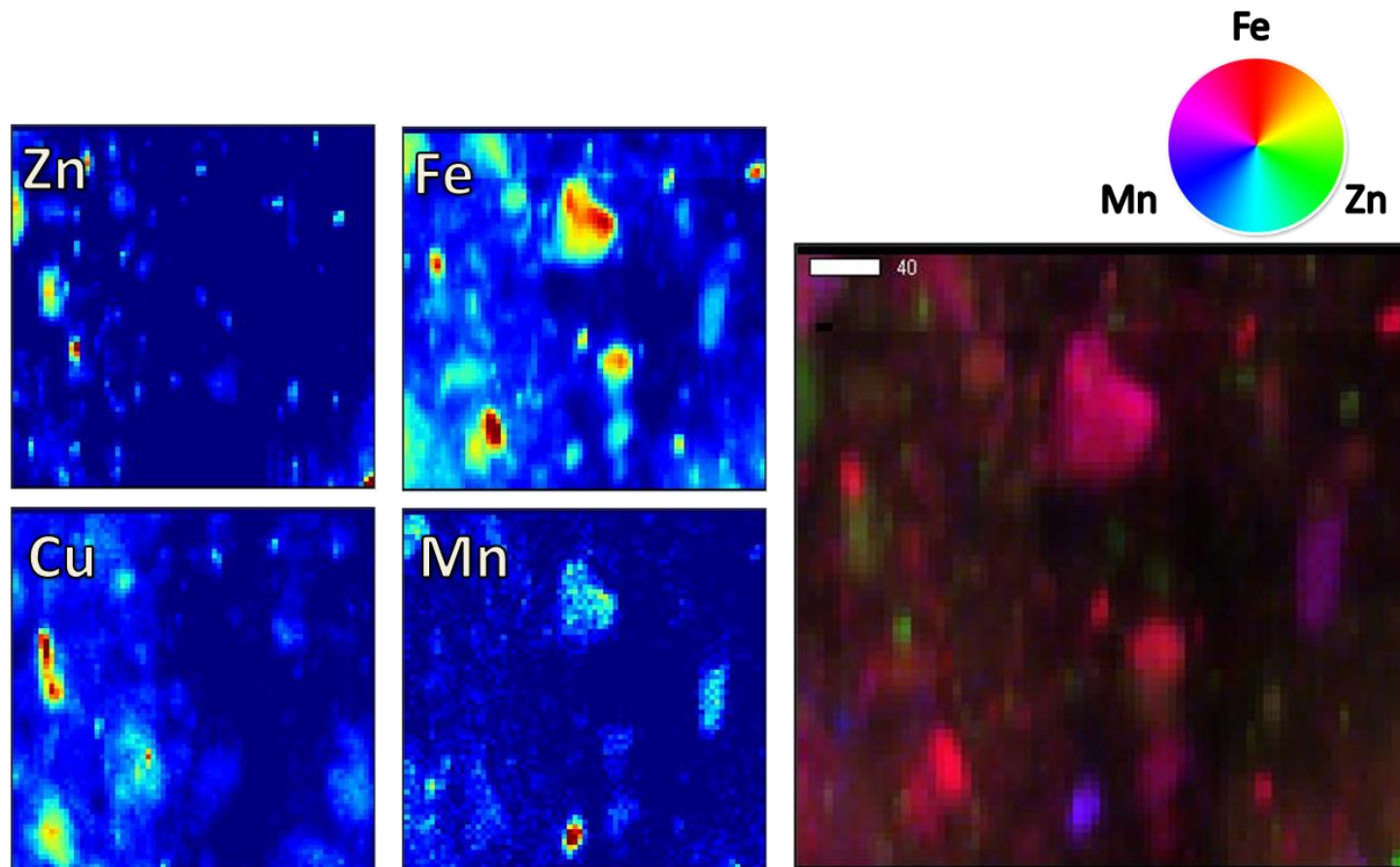


**Fig. C.2.** High erodibility ten years since liming surface soil (0-2 cm) synchrotron XRF microprobe maps for Zn, Fe, Cu, and Mn. Colors denote intensity (red = high relative elemental concentration, dark blue = low relative elemental concentration) and tri-colour maps ( $400 \times 400 \mu\text{m}$ ) reveal 2D spatial relationships of Zn, Fe, and Mn throughout the soil.

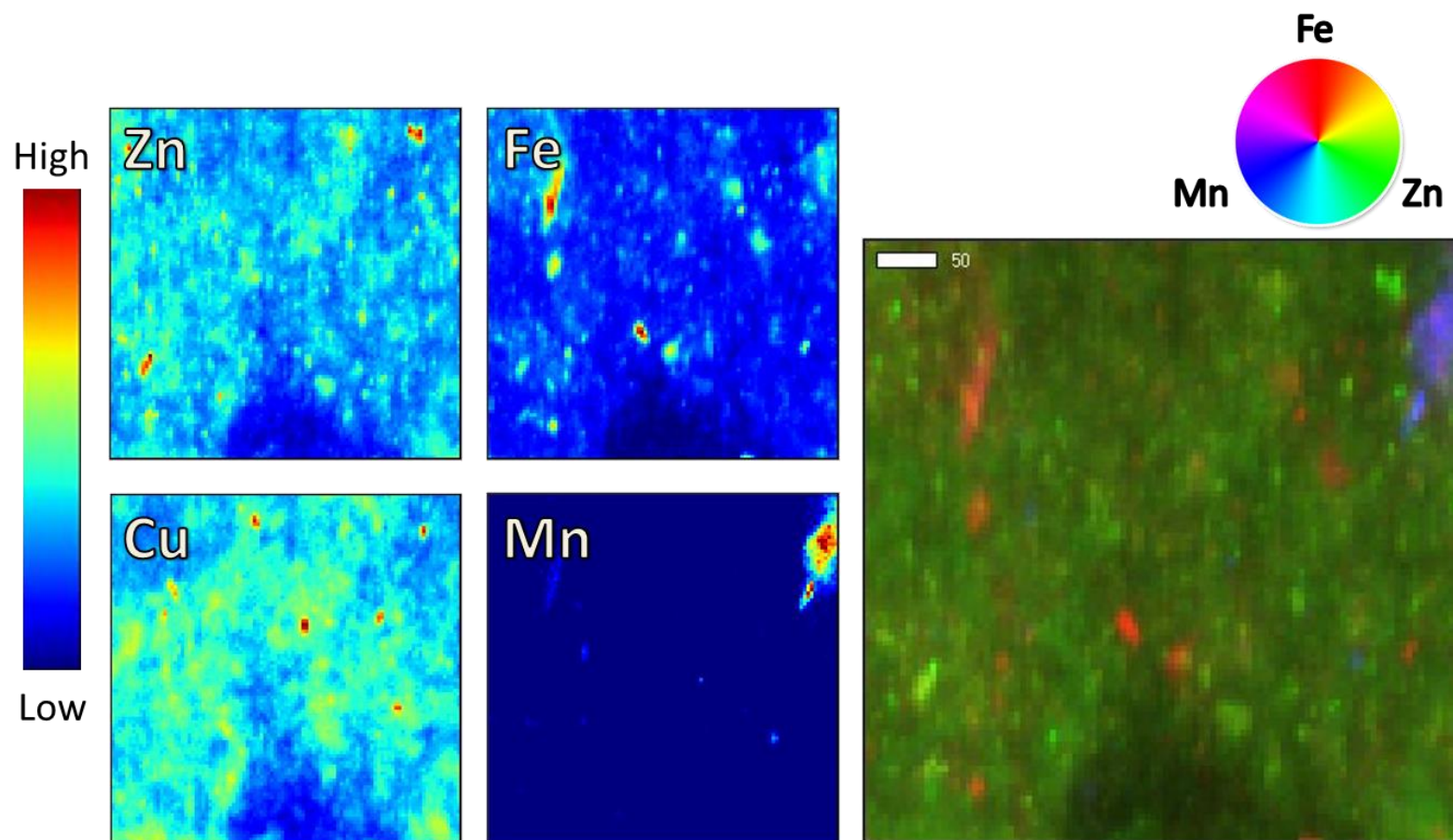


**Fig. C.3.** Un-limed stabilized surface soil (0-2 cm) synchrotron XRF microprobe maps for Zn, Fe, Cu, and Mn. Colors denote intensity (red = high relative elemental concentration, dark blue = low relative elemental concentration) and tri-colour maps ( $500 \times 500 \mu\text{m}$ ) reveal 2D spatial relationships of Zn, Fe, and Mn throughout the soil.